Journal of Archaeological Science: Reports 72 (2026) 105774

Contents lists available at ScienceDirect

Journal of Archaeological Science: Reports

journal homepage: www.elsevier.com/locate/jasrep

The application of quartzite petrogenesis in Palaeolithic research: Methodological basis, ongoing narratives, future directions☆

Alejandro Prieto [a,b,*], Noora Taipale [c,d], David Álvarez-Alonso [e], Esteban Álvarez-Fernández [f], Javier Baena-Preysler [g], Dries Cnuts [c], Ronè Oberholzer [c], Andreas Pastoors [h], Veerle Rots [a,b]

[a] Institut d'Arqueologia de la Universitat de Barcelona (IAUB), Universitat de Barcelona, C. Montalegre 6-8, Soterrani, 08001 Barcelona, Spain
[b] Seminari d'Estudis i Recerques Prehistòriques (SERP), Universitat de Barcelona, C. Montalegre 6-8, Soterrani, 08001 Barcelona, Spain
[c] TraceoLab, University of Liège, Place du 20-août 7, 4000 Liège, Belgium
[d] F.R.S.-FNRS, Brussels, Belgium
[e] Department of Prehistory, Ancient History and Archaeology, Complutense University of Madrid / UCM Research Group "Territorios y sociedades prehistoricas del interior peninsular 971079", Spain
[f] GIR PREHUSAL Departamento de Prehistoria, Historia Antigua y Arqueología, Facultad de Geografía e Historia, C. Cerrada de Serranos s/n., 37002 Salamanca, Spain
[g] Departamento de Prehistoria y Arqueología, Universidad Autónoma de Madrid, Facultad de Filosofía y Letras, Ciudad Universitaria de Cantoblanco, C. Francisco Tomás y Valiente, 1, 28049 Madrid, Spain
[h] Institut für Ur- und Frühgeschichte, Kochstr. 4/18, 91054 Erlangen, Germany

ARTICLE INFO

Keywords:
Non-flint resources
Quartzite
Petrography
Thin Section
Stereomicroscopy
Petrogenesis
Scanning Electron Microscopy

ABSTRACT

Archaeologically-oriented petrography has changed the way of conceiving economic and social practices during the Palaeolithic. Research on quartzite, the second most widely used lithic resource, has experienced a notable increase thanks to the formal definition of the material, methodological improvements, and case studies that are shedding light on the economy and social interactions during the Palaeolithic. This paper briefly presents the progress made during the last years by our research team, particularly in quartzite petrology, together with some thoughts about its future evolution. These advances are based on the petrography of the material and particularly on the application of petrogenesis (a research field in geology that deals with the origin and transformation of rocks) to establish reliable and universal types that are useful for understanding quartzite from a geo-archaeological perspective. Furthermore, we present preliminary results derived from the application of scanning electron microscopy in quartzite petrogenesis. Finally, we propose some perspectives and methodological advances to continue untangling the prehistoric knowledge enclosed in quartzite artefacts.

1. Introduction

Archaeologically-oriented petrography has reshaped our view of Palaeolithic economic and social structures by providing new approaches to archaeological assemblages (e.g., Arrizabalaga et al., 2014; de la Peña et al., 2022; Eren et al., 2014), insights into human behaviours (e.g., Gómez de Soler et al., 2020; Sánchez de la Torre et al., 2020; Vaquero et al., 2019), and revised historical paradigms (e.g., Barkai and Gopher, 2009; Delvigne et al., 2019; Knutsson et al., 2016; Maier et al., 2022; Tarriño et al., 2016). Geoarchaeological techniques have been particularly applied to flint techno-complexes and their potential provisioning areas. Among others, this has allowed archaeologists to trace mobility routes (e.g., Belmiro et al., 2025; Prieto et al., 2016; Sánchez de la Torre et al., 2017), depict raw material acquisition systems (e.g., Calvo and Arrizabalaga, 2020; Fernandes et al., 2008; Ortiz and Baena, 2016), and delve into the technological management of raw materials (e.g., Arrizabalaga et al., 2014; Eixea et al., 2020; Mayor et al., 2022; Rios-Garaizar, 2020). Obsidian studies have also benefitted from the well-understood petrological and geochemical signatures, shedding light on long-distance mobility across the Mediterranean, the Caspian and the

☆ This article is part of a special issue entitled: 'INSTONE' published in Journal of Archaeological Science: Reports.

* Corresponding author at: Institut d'Arqueologia de la Universitat de Barcelona (IAUB), Universitat de Barcelona, C. Montalegre 6-8, Soterrani, 08001 Barcelona, Spain.

E-mail addresses: alejandro.prieto@ub.edu (A. Prieto), noora.taipale@uliege.be (N. Taipale), david.alvarez@ucm.es (D. Álvarez-Alonso), epanik@usal.es (E. Álvarez-Fernández), javier.baena@uam.es (J. Baena-Preysler), dries.cnuts@uliege.be (D. Cnuts), rone.oberholzer@uliege.be (R. Oberholzer), andreas.pastoors@fau.de (A. Pastoors), veerle.rots@uliege.be (V. Rots).

https://doi.org/10.1016/j.jasrep.2026.105774
Received 31 October 2025; Received in revised form 28 March 2026; Accepted 15 April 2026
Available online 29 April 2026

Black Sea (e.g., Cann and Renfrew, 1964; Doronicheva and Shackley, 2014; Orange et al., 2021; Zilhão et al., 2021).

Quartzite was the second most common lithic resource used by Palaeolithic societies, being especially relevant in certain regions such as the Iberian Peninsula, Central Europe, East Africa and the Indian subcontinent, where this rock was the main abiotic resource in old chronologies (e.g., Floss, 1994; Yezad, 2023; Prieto et al., 2021; Soto et al., 2020; Tarriño et al., 2023; Viallet et al., 2024). This makes quartzite an extraordinary proxy for past human activities, especially in areas in which it was the only available raw material, but also in regions and chronologies in which it was used alongside other lithic raw materials (Ebright, 1987; Prieto et al., 2021; Sternke, 2007; Villeneuve et al., 2019).

Quartzite has not experienced similar research interest as chert or obsidian because of its scarcity in areas with a long history of intense archaeological research (e.g., Dordogne, France), the petrological complexity of the rock, and the inherent historiographical limitations (Ebright, 1987; Prieto et al., 2022a, 2021; Sternke, 2007). In recent years, scientific efforts have been made to understand this material through archaeologically-oriented petrography, and they are shedding light on distinct but related behaviours: acquisition systems, technical traditions and specific human activities (Cristóbal et al., 2025; Ebright, 1987; Favreau et al., 2020; Legg et al., 2020; Pedergnana et al., 2017; Prieto, 2018; Prieto et al., 2022b; Roy et al., 2017; Sherman et al., 2024; Sjölander et al., 2024; Soto et al., 2020). The current research dynamic also involves approaches where quartzite is being investigated alongside other exploited lithic raw materials following adapted geoarchaeological approaches (e.g., Abrunhosa et al., 2019; de Lombera-Hermida and Rodríguez-Rellán, 2016; McHenry and de la Torre, 2018; Nash et al., 2022; Prieto et al., 2022a; Schmidt et al., 2024).

This paper puts together the advances our research team has made in archaeologically-oriented quartzite petrography during the last eight years in different archaeological contexts. We additionally discuss the development of the discipline. In addition, we present the first results of a pilot collaborative study employing scanning electron microscope (SEM) analysis that aimed to test the possibilities of this instrument in quartzite petrogenetic analysis and to deepen our understanding of the features that characterise different types of quartzite. SEM has been previously demonstrated to facilitate the understanding of wear formation on different quartzites, and our objective here was to reinforce the previously described petrogenetic classification scheme (Pedergnana et al., 2017, 2018). Our study produced robust results and opened new perspectives on the interaction between quartzite petrogenesis and use-wear formation to be explored in future.

2. Background

2.1. Quartzite petrology

Most geological textbooks define quartzite as a hard, non-foliated metamorphic rock that was originally a pure quartz sandstone (e.g., Allaby, 2013; Tarbuck et al., 2005; Yardley et al., 1990). Unfortunately, the observation of the metamorphic features in stones separated from their bedrock stratum is not easy, especially if only macroscopic observation is performed. In two connected papers, Skolnick (1965) and Howard (2005) refer to this "problem" and address the macroscopic characterisation of quartzites, attending to their granular texture, their ability to present conchoidal fracture, their permeability, their vitreous (sometimes dull) lustre, and their hardness (Fig. 1). A key issue is that metamorphic and sedimentary geneses can produce similar characteristics, raising the question whether these two origins can be distinguished based on macroscopic observation.

According to Skolnick (1965), quartz-arenites or sandstones that have a sedimentary origin are permeable, thereby allowing to distinguish them from metamorphic quartzites. Furthermore, fracture in quartz arenites propagates through the cement, without grain breakage. In contrast, in metamorphic quartzite, the propagation waves pass through the grains, creating a more conchoidal and predictable fracture. Nevertheless, sedimentary quartzites that have been indurated by syntaxial quartz cement can also break through the grain. Howard (2005) recovered the term "orthoquartzite", originally coined to refer to "sandstones" or "quartzitic sandstones" with quartz content over 95% (Krynine, 1948; Pettijohn, 1954), to refer to these "pressure-solution quartzites" (Skolnick, 1965), separating them from quartz-arenites (Folk, 1974). Consequently, quartzite is still a debated topic in geological literature, and despite the formal definition being clear, macroscopic or field observation does not allow for a proper description of these rocks.

The term 'quartzite' has also been applied to describe quartz, particularly in Eastern African Stone Age contexts, as recently highlighted by Tarriño et al. (2023). These rocks or minerals, which the authors refer to as "crystalline quartz-rich raw material" (CQRM), have a macroscopic appearance that resembles metamorphic quartzites in that they represent a "light-coloured, homogeneous, and anisotropic siliceous crystalline material that exhibits a penetrative foliation with a well-defined mineral/stretching lineation" (Tarriño et al., 2023). These minerals do not, however, petrographically show any primary sedimentary origin. They are instead different types of quartz formed as either hydrothermal veins and dykes or as metamorphic rocks exclusively composed of quartz and hosted in quartzite-bearing strata. This debate further illustrates the complexity of quartzite/quartz petrology and the challenges involved in the non-destructive characterisation of quartz-rich rocks.

2.2. Petrogenesis as a basic tool

Petrogenesis is a research field in geology that deals with the origin and transformation of rocks (Bucher, 2023). It is used to describe processes pertinent to the three rock types that can be found on the Earth's surface (igneous, metamorphic and sedimentary rocks). It helps geologists understand the rock cycle and the transformation of different rocks into new ones. A clear example of this is the petrogenesis of shale and its successive transformation towards migmatite as a consequence of progressive metamorphism brought on by an increase in pressure and temperature (Tarbuck et al., 2005). Fig. 2 shows how shale, a clastic sedimentary rock consisting of clay mineral particles, is transformed through successive stages (slate, phyllite, schist and gneiss) into migmatite. This process alters not only the mineralogy of the sample, but notably its texture, particularly as observed macroscopically.

In recent years, quartzites from archaeological contexts have been characterised through thin-section petrography (Prieto et al., 2019, 2024b). After having characterised the homogeneity, textures –*i.e.* the relationship between the particles that compose a rock (Tarbuck et al., 2005)- and packing –*i.e.* the distribution of grains and intergranular spaces in a sedimentary rock (Castro, 1989)- of quartzite thin sections, quantified particular features of the quartz grains (e.g., syntaxial overgrowth, recrystallised grains), measured their orientation, size and morphology, and identified non-quartz minerals, we were able to propose a classification scheme for quartzite consisting of nine types and three groups that reflect the petrogenesis of the material.

Furthermore, these types and groups have been recognised following a non-destructive microscopic approach using stereomicroscopes and microscopic cameras (e.g. Dino-Lites) (Prieto et al., 2020, 2024b). This multiscale methodology combines macroscopic criteria (*i.e.* lustre and density of surface microcracks) and observation of quartzite surfaces under up to 250 × magnification to define textures and packing, to outline visible quartz grain features, to determine grain size and morphology, and to understand the orientation of the particles in order to link each quartzite surface to a particular petrogenetic type. The resulting nine types illustrate the effects of the successive increase in pressure and temperature on the original quartz sandstone, and they also reflect the variability of the material termed quartzite: quartz-arenites

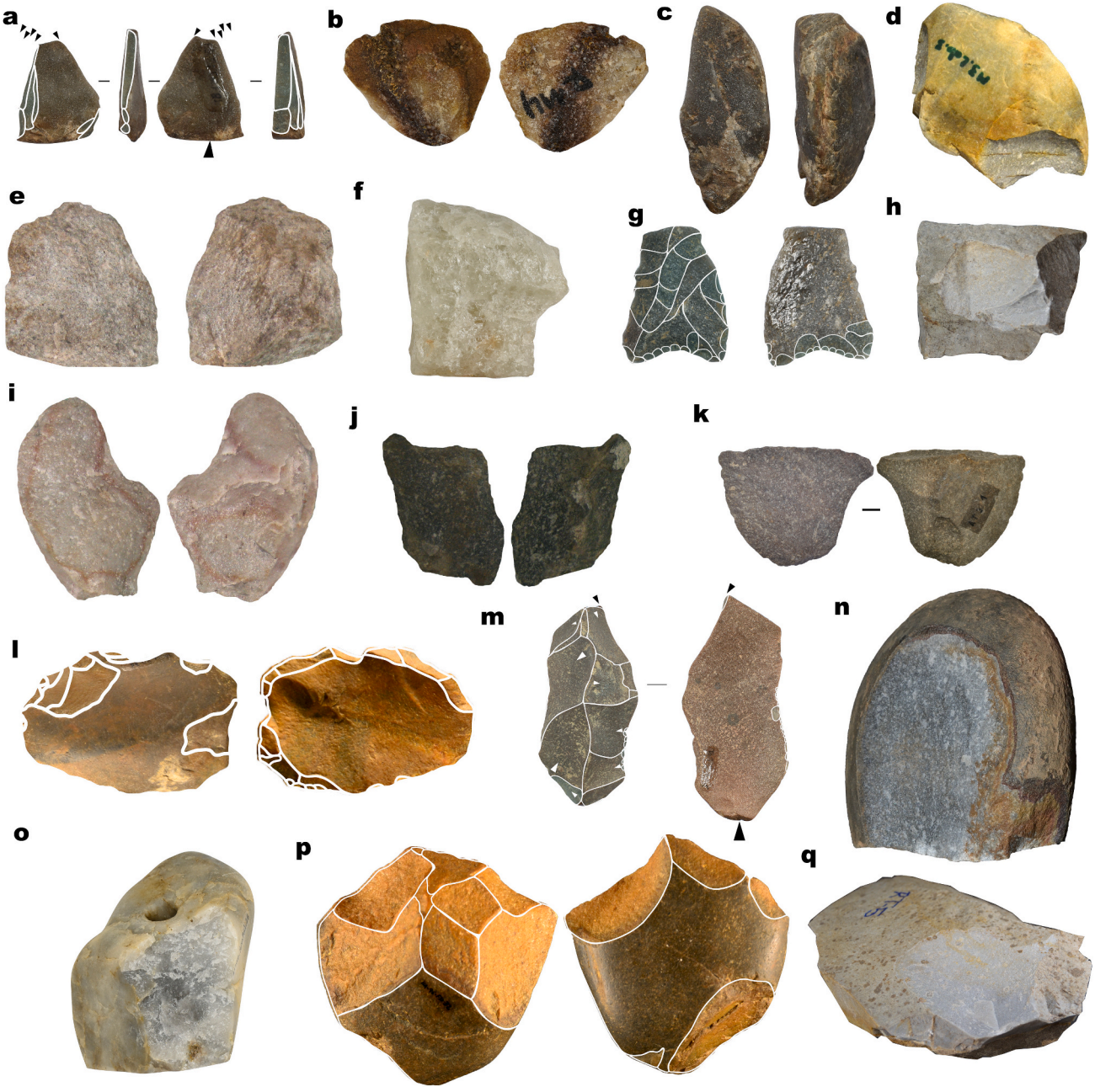

Fig. 1. Quartzite variability expressed in macroscopic pictures of the material analysed in archaeological and geological contexts in the Cantabrian Region, Central Iberia, Arabia, and Central Europe (images not scaled). a) Burin with multiple facets on proximal flake fragment on an RQ type with conglomerate cortex -Level 1c2 (Lower Magdalenian) of *Área de Estancia* at Tito Bustillo cave (Asturias, Spain). b) Geological sample from the Arabian Peninsula, MA type with microcrystalline cement. c) Hammerstone made on an MQ type taken from a conglomerate -Level 1c2 (Magdalenian) of *Área de Estancia* at Tito Bustillo cave (Spain). d) Sample of white OO type quartzite, showing internal unidirectional joints and a well-developed fluvial cortex. Collected at the Deva River (Cantabrian Region, Spain). e) Flake with centripetal removals on a CA type with slight presence of cement -Level XXII-R (Mousterian) of El Esquilleu (Cantabria, Spain). f) Polycrystalline quartz from Naibor Soit (Tanzania). g) Proximal fragment of a concave-based Solutrean point made on SO type (folded variety), characteristic of the Sella valley -Level H1 (Upper Solutrean) from El Cierro cave (Asturias, Spain). h) Sample of an MA type with clayey matrix obtained in the surroundings of the city of Troisdorf (North Rhine-Westphalia, Germany). Microcrystalline cement is completely absent. i) Cortical flake of an OO type procured in a river bank -Level XXII-R (Mousterian) of el Esquilleu (Cantabria, Spain). j) Core flank made on an OO type (medium grained size with oxides and pyrites variety) procured in a conglomerate -Level XXII-R (Mousterian level) of El Esquilleu (Cantabria, Spain). k) Cortical flake of an OO type (fine-grained variety) with more than three extractions, procured from a fluvial deposit -Mousterian level at El Arteu (Cantabria, Spain). l) Levallois core with two platforms made on a BQ type procured from a conglomerate in the Remoña formation -Mousterian level at El Habario (Cantabria, Spain). m) Burin made on a crested blade of an OO type with medium-sized quartz grains -Level 1c2 (Lower Magdalenian) of *Área de Estancia* at Tito Bustillo (Spain). n) Sample of a SO type obtained from the Remoña conglomerate formation in the Cantabrian Region (Cantabria, Spain). It is a dark variety with abundant pyrite and iron oxides. External surfaces are clearly altered by conglomerate cement, forming inner concentric rims. o) AQ sample hosted in the CENIEH Qlithotheque from the Iregua river (La Rioja, Spain). p) Irregular core made on BQ type, originally a white to colourless variety with medium-sized quartz grains. The core was weathered by clay derived from the conglomerate cortex of the Remoña formation -Mousterian level at El Habario (Cantabria, Spain). q) Quartzite sample collected near Troisdorf (North Rhine-Westphalia, Germany), showing an MA part with microcrystalline cement and an OO facies on the same block. Patina does not permit a distinction between the two until the rock is flaked.

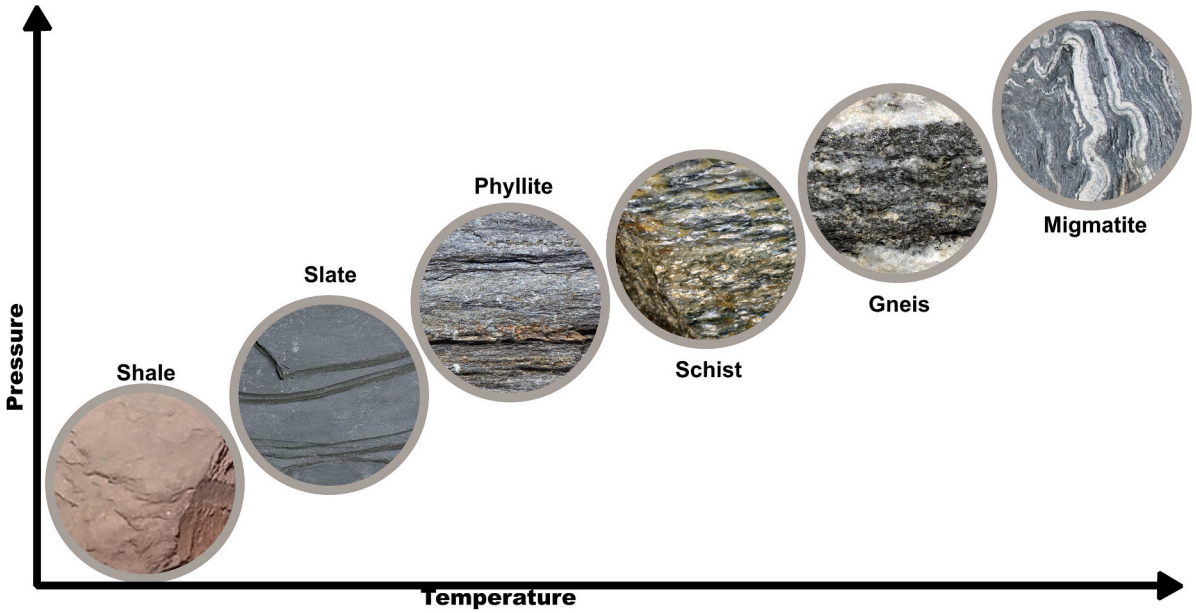

Fig. 2. Schematic representation of the petrogenesis of the shale until it is converted into a migmatite.

–sandstones indurated by compaction and cementation-, ortho-quartzites –deformed sandstones-, and quartzites *sensu stricto*. Fig. 3 presents the petrogenetic scheme proposed, and the processes that produce the features observed in thin section petrography and in non-destructive characterisation are discussed in the following paragraphs and summarised in Table 1.

Quartz-arenites form through sedimentary processes that indurate accumulated clastic particles (mainly silica, 0.062 – 2.0 mm ø). Depending on the environment where these particles were accumulated, quartz-arenites can be homogeneous or heterogeneous with regard to particle size, morphology and mineralogy (monocrystalline or poly-crystalline clastic grains) and also variable in their texture. In some specimens, it is possible to observe post-depositional weathering of quartz grains. Therefore, quartz-arenites can be either homogeneous or heterogeneous regarding their main and secondary grain framework, and they generally show sedimentary markers such as stratification/bedding –layering deriving from the deposition of particles (Folk, 1974)- or even ripple structures –wavy sedimentary structures (Adams et al., 1988). Quartz-arenites can be consolidated by cement that binds together quartz grains or by burial processes in which quartz grains and matrix fill the spaces between them. When the quantity of matrix and cement is higher than 5%, they are classified as Matrix/cemented quartz-Arenites (MA type) –*i.e.* immature sandstones (Folk, 1974)-, and when the proportion of matrix or cement is lower than 5%, they are classified as Clastic grained quartz-Arenites (CA type) –*i.e.* submature to mature sandstones (Folk, 1974).

In the first type, **MA,** common features observed in thin section are the association of clastic grained texture and matrix and/or cement in higher proportion than 5%. Generally, packing is floating or punctual and most of the quartz grains are clastic (straight extinction) (Fig. 4). General lustre is earthy, and bedding planes can be observed. Surface micro-cracks are scarce due to the low compaction of the material. When surfaces are observed at the microscopic scale, a saccharoidal (sugar-like) texture is evident, along with floating or point-supported packing and flat to irregular grain outlines, the latter indicating the presence of a matrix or cement in angular to rounded quartz grains. It is easy to recognise individual grains, although this can be hindered by the matrix or non-quartz cement. Generally, the MA type fractures around quartz grains; only in specific cases where chalcedonic or microcrystalline quartz cement binds the grains do both cement and grains become

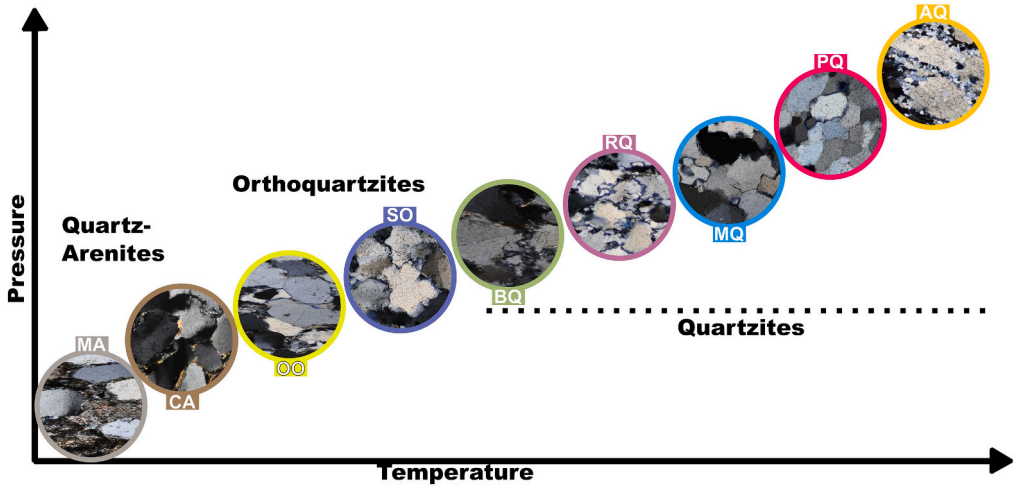

Fig. 3. Schematic representation of the petrogenesis of quartzites.

Table 1
Main features identified in each of the petrogenetic types following thin section, stereomicroscopic, and digital microscopic analysis. -, +, ++, +++ are used to describe the presence of relative frequency of features, corresponding to anecdotical, minor, abundant and major, respectively.

	Thin section		Stereomicroscope	
	Low magnification	High magnification	Low magnification	High magnification
MA	Clastic-grained	Straight extinction on grains	Earthy lustre	Visible grains +++
	Floating-Punctual pack.	weathered grains	Sacharoidal texture	Grain coatings ++
		Matrix/cement ++	Floating-puntual pack	Matrix/cement ++
CA	Clastic-grained	Straight extinction gr.	Vitreus lustre +	Visible grains +++
	Tangential-complete pack	Matrix/cement -	Granular texture	Grain coatings +
			Tangential-complete	Matrix/cement -
OO	Clastic-grained	Overgrowths ++	Compact & grainy	Visible grains ++
	Tangential-complete pack	Concave-convex limits	Microcracks ++	Overgrouths ++
		Undulose extinction +	Vitreus lustre ++	Microcracks ++
SO	Clastic-grained	Sutured/ microstylolitic ++	Fine but grainy text.	Visible grains +
	Complete-sutured pack.	Undulose extinction +++	Microcracks +++	Thin & ruffle grain limits
		Böhm lamellae	Vitreous lustre +++	Microcracks +
BQ	Mortar texture	Sutured/ microstylolitic ++	Fine texture	Visible grains -
	Sutured packing	Undulose extinction +++	Microcracks +++	Thin & ruffle grain limits
		Recrystallised grains ++	Vitreous lustre +++	
RQ	Mortar texture	Sutured/ microstylolitic +	Soapy texture	Almost no grains
	Sutured packing	Undulose extinction ++	Microcracks +	Thin & ruffle grain limits
		Recrystallised grains +++	Vitreous lustre +++	Blurry outlines
MQ	Foam texture	interdigitated grain +++	Soapy texture	No grain detected
	Lobated grain boundaries	straight triple 120° +	Microcracks -	Blurry outlines
			Translucent	
PQ	Foam texture	straight triple 120° +++	Soapy texture	No grain detected
		Euhedral quartz grains	Microcracks -	Blurry outlines
			Translucent	
AQ	Foam texture	straight triple 120° +++	Vitreous lustre +++	Microcracks +
	Chessboard texture	Abnormal coarse grain	Fine texture	Visible grains +
			Microcracks ++	

fractured (Prieto et al., 2021d). This type mainly corresponds to immature sandstones as defined by Folk (1974).

For the second type, the **Clastic grained quartz-Arenite**, common features observed in thin section include the association of a clastic-grained texture −composed of identifiable rock or mineral fragments in a proportion higher than 95%-, tangential to complete packing, and the presence of clastic quartz grains (Fig. 4). Lustre starts to change towards vitreous and surface microcracks increase due to the higher compaction of the material. The lower quantity of cement or matrix also makes fracture more controlled, but still frequently around the grain. This is observed in the less rugged (granular) texture and the reduced quantity of secondary matrix or cement. As with the previous type, it is possible to recognise the outlines of the grains and their original rounded or angular morphologies that can also be slightly weathered. This type mainly corresponds to mature sandstones in Folk's (1974) classification.

Orthoquartzites form as a consequence of deformation processes that occur without metamorphism (as indicated by the lack of recrystallised grains) but related to it: pressure-solution cementation and plastic deformation (Bastida, 1982; Folk, 1974; Howard, 2005; Skolnick, 1965; Wilson, 1973). Both processes lead to the induration and compaction of the material through sedimentary processes and/or a low degree of regional metamorphism. These processes modify the original texture of the quartz-arenite but the composition is not clearly altered. Whereas the original quartz-arenite may have been homogeneous or heterogeneous in terms of quartz grain size, morphology and other features, orthoquartzites that derive from them present a higher degree of homogeneity because pressure-solution and deformation transform their constituent particles (Wilson, 1973). Despite compaction being the most relevant feature that defines this group, each of the processes involved characterise each orthoquartzite type. The first process is pressure-solution cementation, and it creates the syntaxially Overgrown Orthoquartzite (OO type). The second is plastic deformation and it creates the Sutured grain orthoquartzite (SO). Generally, the second follows the first one and inherits its features.

Syntaxially Overgrown Orthoquartzite thin sections show a clastic-grained texture, tangential to complete packing and quartz grains that display a characteristic syntaxial cement that grows in optical continuity with the original grain, adapting to the spaces between contiguous grains (Fig. 5). These overgrowths may generate large extensions at the boundaries of the grains with concave–convex planes, making the quartz grains rounder and increasing their size. Undulose extinction −a petrographic phenomenon in which single or multiple quartz grains submitted to similar deformation present a wavy appearance under polarised light (Adams et al., 1988)- is evenly distributed and affects a limited number of quartz grains. These changes represent a more advanced diagenetic stage of dissolution-cementation and/or slight deformation by lithostatic pressure, which is also well observed in the quartzite surfaces. Here, (generally rounded) quartz grains are visible. These rocks break through the silica cement (observed as small whitish halo or as coating around individual grains) or along the contact between quartz grains, developing a compact and grainy surface. This texture is observable in the abundant surface microcracks or squama created as a consequence of a more compact packing in which the propagation wave advances in a stepped but relatively homogeneous way. The vitreous lustre is medium in intensity due to the presence of silica cement and the few deformed grains. This type corresponds to microstructure A in the detrital grain quartzite of Wilson (1973) and the scarcely deformed quartzite of Bastida (1982), modified during diagenesis.

Sutured-grained Orthoquartzite thin sections have clastic-grained texture, complete to sutured packing and quartz grains displaying signs of deformation in the form of sutured/microstylolitic grain limits, massive undulose extinction, and deformation lamellae −Böhm lamellae (Bastida, 1982)- (Fig. 5). The development of these quartz grain features seems to be influenced by the former grain size of the quartz-arenite, with deformation bands being more frequent in homogeneous and coarse-grained quartzites −medium to very coarse sands according to the Udden-Wentworth scale (Wentworth, 1922)- than in heterogeneous and finer-grained quartzites, which are more associated with sutured/microstylolitic quartz grain limits. Importantly, this deformation also produces more angular and elongated quartz grains in the latter type. Many grains still maintain the previous overgrowths despite the characteristic dust lines (original grain borders) starting to erode. The increase in pressure is sometimes observed in the form of a few recrystallised quartz grains (<5% of the thin section) and unidirectional foliation fabric, sometimes detected when quartzite surfaces are

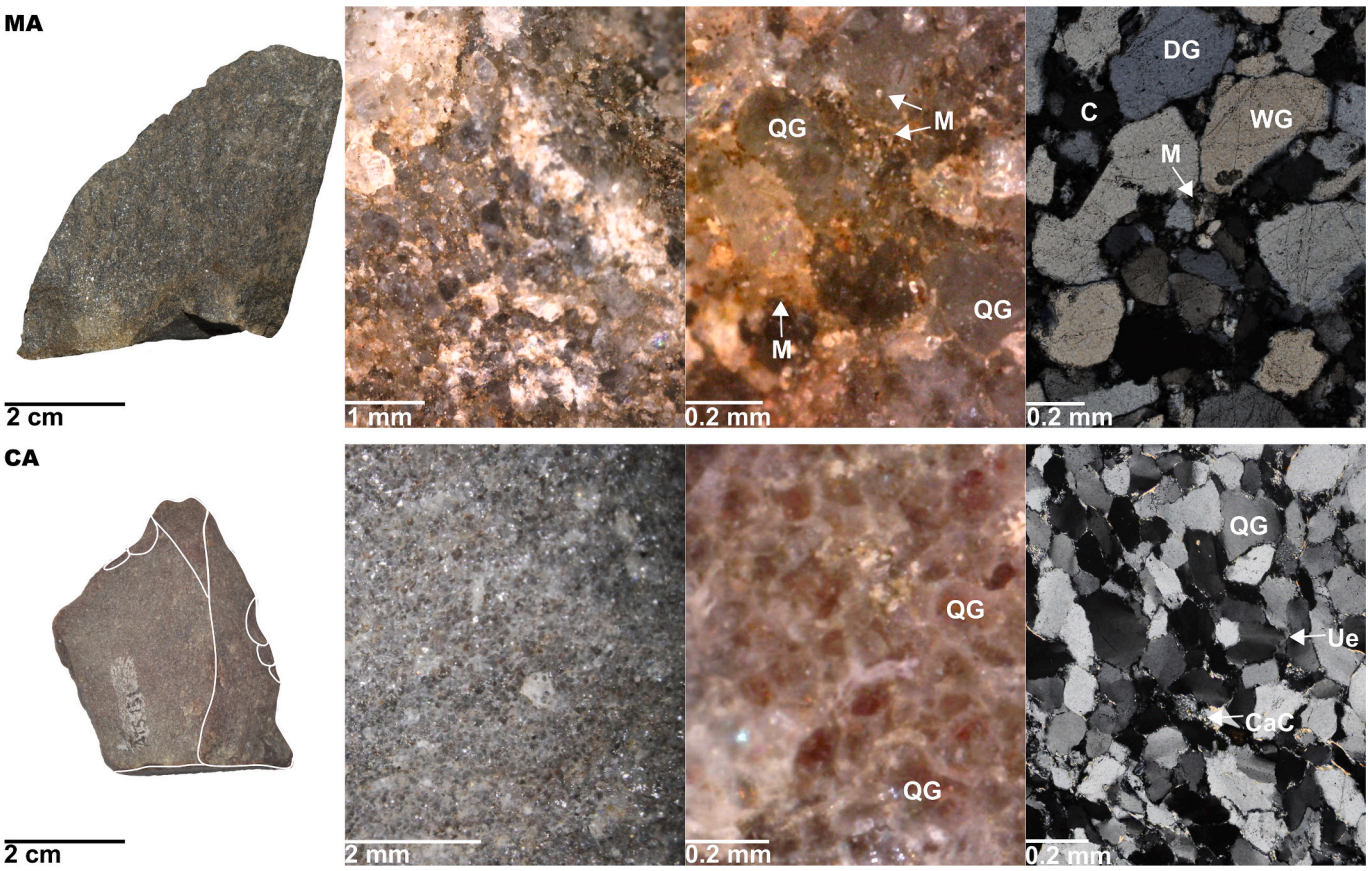

Fig. 4. Composite image presenting an MA (above) and a CA (below) type of quartz-arenite. They correspond to the samples CoB.J26.38.46 -Coimbre (Asturias, Spain), level 6 (Gravettian)- and ATS-151 -El Arteu (Cantabria, Spain), Mousterian level. From left to right, macroscopic picture, microscopic surface picture at 50× digital magnification, microscopic surface picture at 250× digital magnification, and a thin section picture at 100× optical magnification. Note that in MA, quartz grains show ruffled or sinuous outlines due to presence of matrix, whereas grain boundaries in CA are smoother. QG: Quartz grain. M: Matrix. C: Cement. DG: Detrital quartz grain. WG: Weathered quartz grain. Ue: Undulose extinction (not intense and limited to a small number of grains). CaC: Carbonated cement.

observed. Here, the increase in pressure is also reflected in the higher intensity of vitreous lustre (probably related to the undulate extinction), the finer (but still grainy) texture and the high quantity of surface microcracks. The last two features are the consequence of the increase in compaction, caused by the merging of the grains that favours fracture through the grain and hinders the detection of grain boundaries. Still, a few grains can be observed in the form of flat and ruffled grain boundaries or in squama, associated with overgrowths. SO type corresponds to the detrital grain type B of Wilson (1973) and the quartzite with deformed and slightly or non-recrystallized grains of Bastida (1982).

Quartzites *sensu stricto* form through metamorphism. While the previous type can show sporadic evidence of this process by the limited presence of recrystallised quartz grains or deformation lamellae, quartzites *sensu stricto* have undergone a substantial modification of texture caused by increase in pressure and temperature. They have transformed into proper quartzites and display new recrystallised quartz grains (Howard, 2005). The increases in temperature and pressure do not always correlate linearly, promoting, again, some internal variation. Despite the changes, quartzites *s.s.* show features that are remnants of the original sedimentary rock (quartz-arenite or orthoquartzite). Quartzites *s.s.* can be divided into five different types. Transition from one type to another is generally gradual, making it possible to sometimes observe two types on a single specimen. This is particularly the case for the last three types discussed below. The transformations from one type to another are characterised by different recrystallisation regimens (Hirth et al., 2001; Hirth and Tullis, 1992; Howard, 2005; Prieto et al., 2024b, 2019; Skolnick, 1965; Stipp et al., 2002a, 2002b; Wilson, 1973).

Bulging recrystallised Quartzite thin sections are characterised by the association of a mortar texture –partially preserved clastic depositional texture with fine, strain-free crystals along grain boundaries (Howard, 2005)- and sutured packing (Fig. 6). Original grains display sutured or microstylolitic limits, deformation lamellae and clear undulose extinction (Passchier and Trouw, 2005). Some of these grains may display characteristics of the previous types (e.g., syntaxial overgrowth). Recrystallised grains appear as a second grain mode within this type. They are characterised by small size (corresponding to very fine to fine silt) and high sphericity –a measure of how close particle shape is to a perfect sphere *i.e.*, L/W = 1 (Folk, 1974)- and roundness –how angular or spherical a particle is (Folk, 1974)- indices (Skolnick, 1965). The recrystallised grains do not present any sign of deformation and are situated at the boundaries of the original grains, never exceeding 50% of the sample (Stipp et al., 2010; Stipp and Tullis, 2003). This particular texture is formed by grain boundary migration, which generates serrated boundaries (microstylolitic texture). When these boundaries break, new grains form (Passchier and Trouw, 2005; Stipp et al., 2002a). The metamorphic conditions are the consequence of low to medium temperature and low pressure, which generate quartzite surfaces characterised by a fine texture in which only a few quartz grains can be observed. These grains tend to create a sutured packing, and ruffled grain boundaries can be observed on flat quartzite surfaces (unrelated to the presence of matrix and or cement). Moreover, most of the individual grains cannot be discerned. These features reflect an extremely compact material in which the propagation wave breaks through grains, increasing conchoidal fracture (and more predictable fracturing) and reducing the quantity of surface microcracks. Importantly, the latter are more common (even more frequent than in previous types) in quartzites

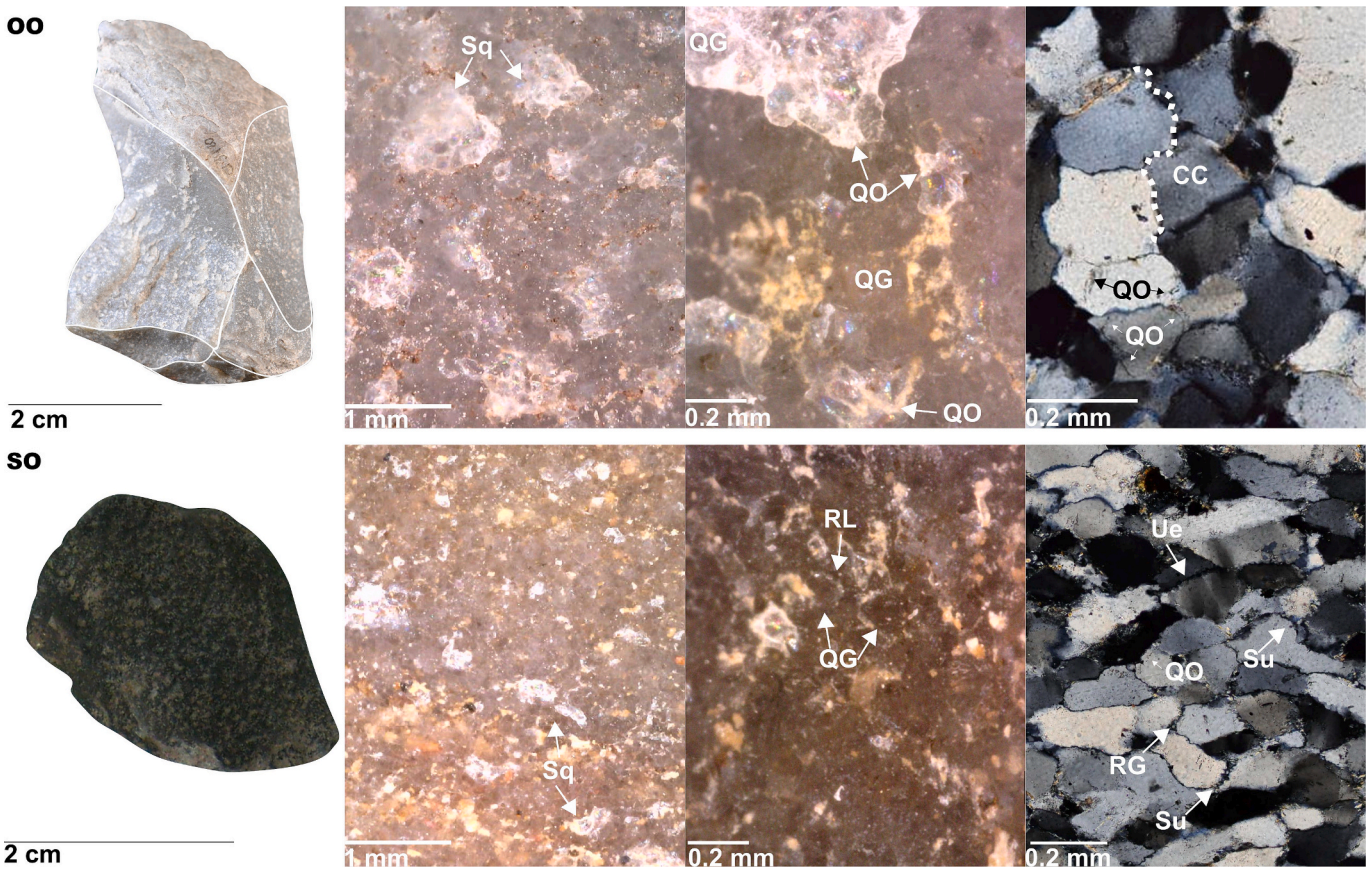

Fig. 5. Composite image presenting an OO (above) and an SO (below) type of orthoquartzite. They correspond to the samples Ci-3420 -El Cierro cave (Asturias, Spain), level G1 (Lower Magdalenian)- and ES-290 -Esquilleu (Cantabria, Spain), level XIII (Mousterian). From left to right, macroscopic picture, microscopic surface picture at 50× digital magnification, microscopic surface picture at 250× digital magnification, and a thin section picture at 200× optical magnification. Sq: Squama or surface micro-crack. QG: Quartz grain. QO: Syntaxial overgrowth (the original outline of the grain (dust lines) and the direction of grain "expansion" as it fills the empty space are marked with arrows). CC: Concave-convex quartz grain limits. RL: Ruffled quartz grain limit. Ue: Undulose extinction. Su: Sutures -sigmoidal shape. RG: Recrystallised grain -new grain developed as consequence of metamorphism.

that possess foliation structures −cleavage, schistosity, or other planar structures in metamorphic rocks (Passchier and Trouw, 2005). This is another signature that reflects the increase of pressure. They correspond to some of the quartzite types with foam texture described by Howard (2005), the microstructure regime 1 of Hirth and Tullis (1992) and the BLG of Stipp et al. (2002a) and Paschier and Throuw (2005).

The second type of *s.s.* quartzite is the **Subgrain Rotation recrystallised Quartzite**, characterised in thin section by mortar texture (with a tendency toward a foam one) and, again, sutured packing (Fig. 6). As in the previous type, there are two distinct grain modes. The first represents the original quartz grains that are in this case even more deformed (generally fractured and not displaying the previous deformation features) but similar to those described for the previous type. The second mode consists of recrystallised quartz grains that are present in higher proportion (> 50%) and are bigger (particle size from fine silt to coarse silt) and less rounded than in the previous type. The latter grains occur as a host of grains around the old grains, but also inside the grains, creating a homogeneous structure. This texture is formed through grain boundary migration accompanied by the rotation of their bulging edges (Howard, 2005; Passchier and Trouw, 2005; Skolnick, 1965; Stipp et al., 2010, 2002a; Stipp and Tullis, 2003). These characteristics derive from an increase in pressure and temperature (400–500 °C). This metamorphic stress produces more compact material, where the propagation wave breaks through the new structure. This is reflected in the quartzite surfaces as soapy texture and limited visibility of quartz grain boundaries in the form of sutures on flat surfaces. Sometimes it is possible to detect blurry areas surrounding grains. The compactness of these quartzites promotes an even more conchoidal and predictable fracture than in the previous type and surface micro-cracks are rare. The lustre, as on the previous type, is vitreous and highly intense as a reflection of this new structure in which the whole rock has been subjected to medium-intensity metamorphism. A few quartzites show foliation structures. They correspond to the types described by Howard (2005) with mortar texture, the microstructure regime 2 of Hirth and Tullis (1992) and the subgrain rotation recrystallisation (SGR) of Stipp et al. (2002a).

In the third type, **grain boundary Migration recrystallised Quartzite**, the texture is completely differentiated from the first two by the presence of an interlobate −irregular lobate grain boundaries (Passchier and Trouw, 2005)- with a tendency towards foam texture in which old and new grains cannot be distinguished (Fig. 6). Here, all grains display similar features, concave-convex and/or interdigitated grain limits (sometimes microstylolitic limits), showing on occasion straight triple 120° points. Metamorphic deformation has here led to the advanced transformation of the grains through recrystallization. Crystals are very heterogeneous in terms of size, morphology and orientation. This is the consequence of an almost full recrystallisation of the quartzite under high temperature conditions (≈500 °C) and the pressure effect that favours very rapid migration of the boundaries and their fracture due to rotation processes. This process generates an extremely compact mass of crystals that favours predictable crack propagation and conchoidal fracture. These conditions are reflected in fracture surfaces with a soapy texture, in which no grain boundaries can be detected even in the rare surface microcracks. Frequently, light penetrates inside the

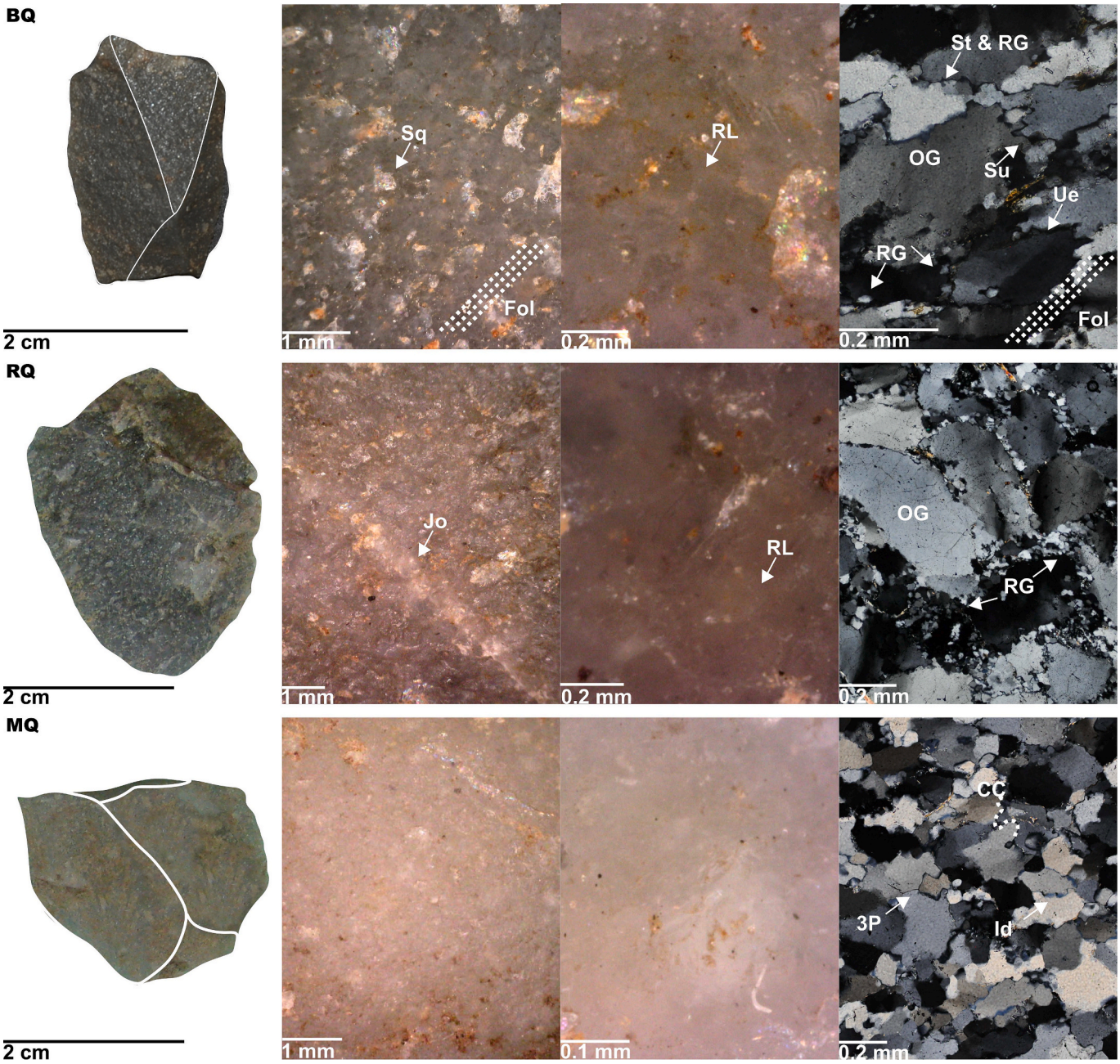

Fig. 6. Composite image presenting a BQ (above), an RQ (middle) and an MQ (below) types of quartzite *sensu stricto*. They correspond to the samples CoB. K26.37.201 -Coimbre (Asturias, Spain), level 6 (Gravettian)-, ES-378 -Esquilleu (Cantabria, Spain), level XIII (Mousterian), and ES-411 -El Esquilleu (Spain), level XIII (Mousterian). From left to right, macroscopic picture, microscopic surface picture at 50× digital magnification, microscopic surface picture at 250× digital magnification, and a thin section picture at 200× optical magnification. Sq: Squama or surface micro-crack. Fol: Foliation structures. RL: Ruffled quartz grain limit. OG: Original quartz grain. St & RG: Microstylolitic quartz grain limit and recrystallised quartz grain. Ue: Undulose extinction. Jo: Joint. RG: Recrystallised quartz grain. CC: Concave-convex quartz grain limits. 3P: 120º Triple points. Id: Interdigitated quartz grain limits.

quartzite, and when rock fragments are relatively thin (less than 1 mm), these quartzites are translucent. They correspond to some of the types of grain enlargement described by Bastida (1982), the microstructure regime 3 of Hirth and Tullis (1992), and the grain boundary migration recrystallisation (GBM) of Stipp et al. (2002a).

Polygonal-grained recrystallised Quartzite has similar features to the previous one, although in this case, the grains display a clear foam texture −granoblastic mosaic of interlocking polygonal and euhedral grains with straight boundaries forming 120° angles and triple junctions (Howard, 2005; Passchier and Trouw, 2005)- (Fig. 7). All grains display a uniformly hexagonal shape. Generally, these quartzites do not have non-quartz minerals, although new muscovite or even a few mica flakes can be distinguished in the quartz grains. These quartzites form at a higher temperature than the previous type and also under higher pressure. Sometimes this type co-occurs with the previous or following ones in the form of deformation bands. However, the compactness of each type and the fact that the original sandstone was transformed under similar high-energy metamorphic conditions mean that the crack propagates uniformly through the different varieties (in opposition to previous types). The characterisation of PQ quartzites using non-destructive methods reveals that they are very similar to the MQ type, hindering their identification. These quartzites correspond to the triformal structure of Howard (2005) and the polygonal grains of Wilson (1973).

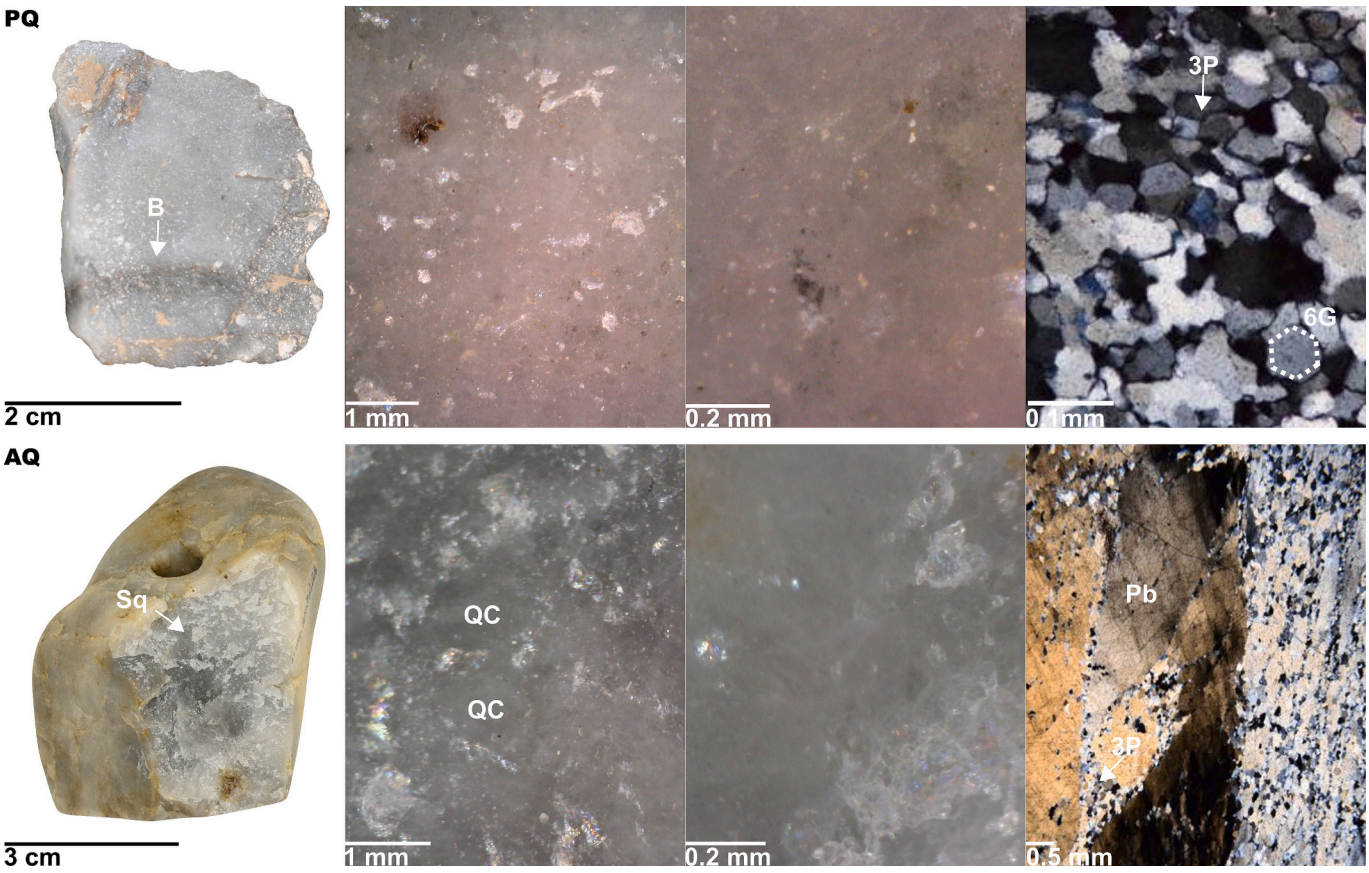

Fig. 7. Composite image presenting a PQ (above) and an AQ (below) types of quartzite *s.s.* They correspond to the samples Ci-55325 -El Cierro Cave (Asturias, Spain), level H (Upper Solutrean) and CENIEH.026 -geological sample from Iregua River (La Rioja, Spain). From left to right, macroscopic picture, microscopic surface picture at 50× digital magnification, microscopic surface picture at 250× digital magnification, and thin section picture at 200× optical magnification. B: Bands of the PQ type. 3P: 120º Triple points. 6G: Hexagonal grains. Sq: Squama or surface micro-crack. QC: Quartz clast. Pb: Porfidoblast

The last type is the **Abnormal coarsening grains recrystallised Quartzite**. Despite still being a quartzite, this type starts to present features resembling pure quartz formed in migmatites or recrystallised under metamorphic conditions (Fig. 7). The main texture is porphyroblastic, in which a few big grains (>coarse sands) are surrounded in a mass of euhedral crystals generally presenting 120° triple point contacts and straight limits. In some specimens, the porphyroblasts maintain at a certain orientation the polygonal structure of the previous type –as a chessboard texture (Passchier and Trouw, 2005; Tarriño et al., 2023). In this case, the temperature and pressure have been even higher than those involved in the formation of the previous type, reaching almost the melting point of silica. Generally, these quartzite surfaces are characterised by their highly intense vitreous lustre and a generally fine texture in which only a few isolated crystals are visible with angular limits in a plain relief. Despite the compactness of the material, the presence of surface microcracks is higher than in the previous two types, probably as a consequence of the porphyroblasts. These quartzites correspond to the abnormal coarsening or the Exaggerated grain growth of Wilson (1973).

3. Materials and methods

To investigate the potential of scanning electron microscopy in quartzite characterisation and to deepen our understanding of the petrogenesis of quartzites, we carried out an exploratory analysis of the first seven petrogenetic types of quartzites discussed above: MA and CA for the quartz-arenites, OO and SO for the orthoquartzites and BQ, RQ and MQ for the quartzites *s.s.* The analysed samples (n = 16) derive from previously characterised quartzites (by thin section petrography and optical stereomicroscopy) that are stored at the University of the Basque Country. They derived from different geoarchaeological campaigns at the Deva, Cares, and Sella valleys (Asturias and Cantabria, Spain) and from the Lower Rhine Valley (North Rhine-Westphalia, Germany). Quartzites from the following archaeological sites were also included: El Arteu, El Habario, El Esquilleu, Coimbre, El Cierro and Troisdorf-Ravensberg (Martín-Jarque et al. 2023, Prieto 2018; Prieto et al. 2019, Prieto et al., in press, 2021c, 2021d, 2023).

We used a scanning electron microscope JEOL IT300 (EDX detector JEOL ex-230) to analyse fresh fracture surfaces of 16 quartzite samples. They were cleaned for analysis by ultrasonicating them in pure acetone for c. 5 min and then air-dried, repeating the procedure when necessary. All samples were analysed uncoated. The images were acquired in low vacuum mode (30 Pa) using the secondary electron detector (LVSED) at 15–20.0 kV with a probe current (PC) of 60.0 and magnification range from 100 × to 900 × . Image contrast and brightness were adjusted afterwards in Photoshop (version 27.4.0) to optimise visibility.

The benefits of using secondary electron imaging in LVSED mode include the high resolution and excellent topographic contrast it provides, the non-destructive nature of the analysis that allows linking features observed in thin section to structures visible on fracture surfaces, and the superior ability to reveal surface relief and three-dimensional structures on rough, irregular fracture surfaces that can be challenging to examine with optical microscopy.

4. Results: Petrogenesis observed with scanning electron microscopy (SEM)

Figs. 8, 9, 10 and 11 present the images acquired for the seven quartzite types (MA, CA, OO, SO, BQ, MQ, RQ). Fig. 8a shows the

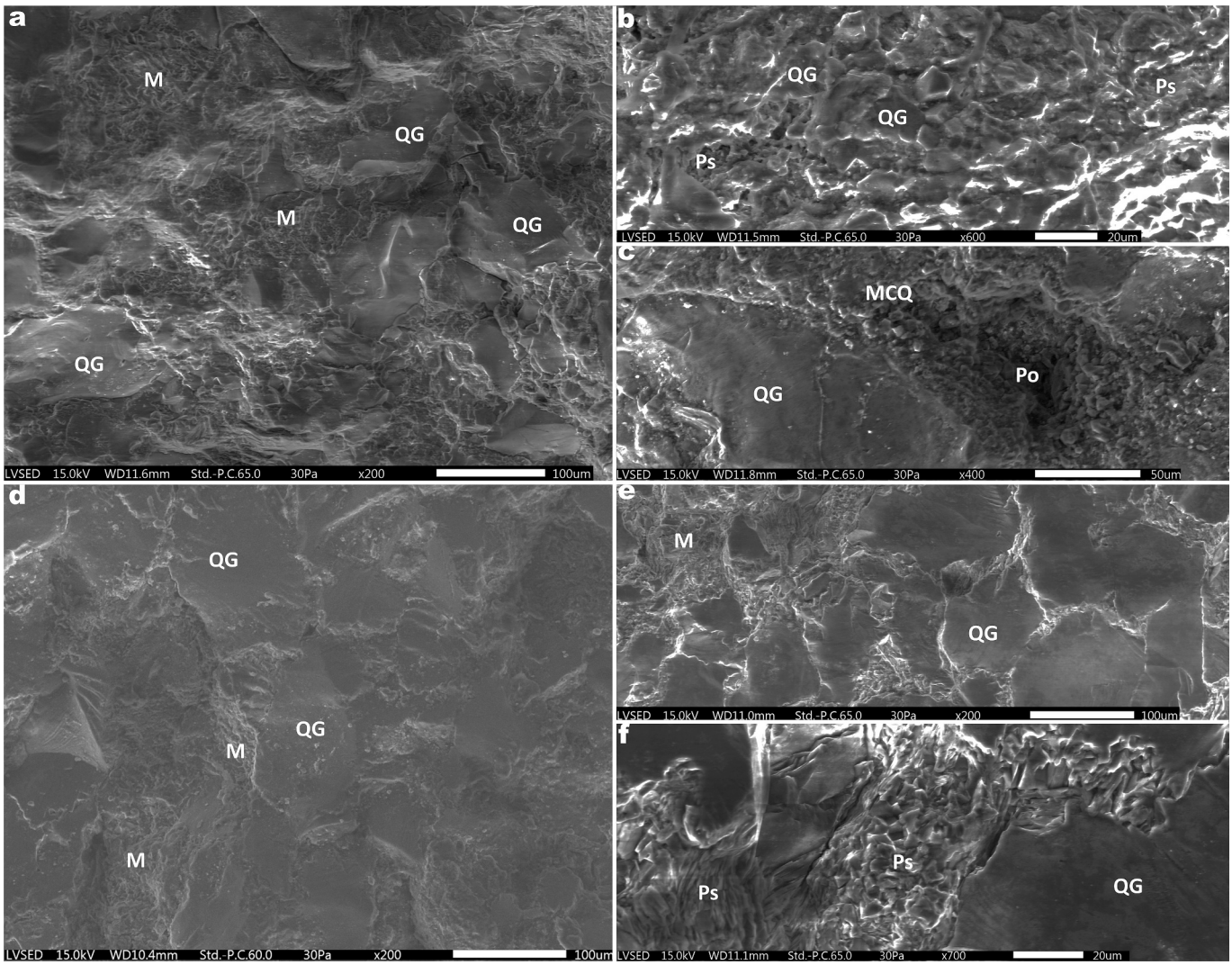

Fig. 8. Surfaces of MA and a CA quartz-arenites observed with the SEM: a) Textural picture (200x) of DC-03-02, a MA type with clayey and siliceous matrix. Sample collected at a fluvial deposit in the Deva-Cares valley. b) Detailed picture of the matrix in sample DC-03-02 showing small detrital quartz grains and phyllosilicates. c) Detailed picture (400x) of Tr-223-3-2 showing a quartz grain surrounded by microcrystalline/chalcedonic quartz cement filling the space between this and other quartz grains. Sample from the Mousterian level of Troisdorf-Ravensberg, North Rhine-Westphalia, Germany. Middle Palaeolithic. d) Textural picture (200x) of ATS-151, a CA type with small relicts of matrix. Sample from the Mousterian level of El Arteu, Cantabria, Spain. e) Picture (200x) of ATS-151, a CA type showing higher quantity of matrix. f) Detailed picture (700x) of ATS-151, showing the matrix consisting of phyllosilicates. M: Matrix. QG: Quartz grain. MCQ: Microcrystalline quartz cement. Po: Pore; Ps: Phyllosilicates.

general texture of the MA types, in which the presence of matrix is clear, together with a marked relief derived from the extraction of complete quartz grains (but note also fracture through the grain). On this sample, detrital quartz grains surrounded by considerable masses of matrix (composed of quartz grain matrix and clay) are clearly visible (Fig. 8a-b). Fig. 8c presents another quartz-arenite, in this case, with chalcedonic cement −characterised by their fibrous and microcrystalline habit. This cement partially fills the pores between weathered quartz grains and produces a texture similar to those described for quartzite from Belgium (Blomme et al., 2012; Cnudde et al., 2013; Veldeman et al., 2012). The texture of a CA sample is shown in Fig. 8d. Here, the quantity of matrix is notably reduced, and it is mainly visible as scarce holes that probably represent single detrital quartz grains that were plucked out when the stone was flaked. Fig. 8e shows how grains are bound together thanks to a matrix composed of weathered phyllosilicates, presented in detail in figure 8f.

Fig. 9 shows the two types of orthoquartzites in which reliefs are gentler but stepped because both grains and matrix are broken by the wave impact. In Fig. 9a-b, we can easily observe the concave-convex packing of (fractured) grains that results in a relatively flat fracture surface relief characteristic of OO type quartzite. This structure presents the syntaxial overgrowths detected in thin section, visible in most of the quartz grains in Fig. 9b and 9c. The latter image shows how the empty spaces between the grains are filled by the syntaxial overgrowths. However, further research efforts are necessary to properly detect them and to understand their visual appearance in SEM images, as well as their role in the homogeneity of the material and their interaction with the original secondary matrix and/or cement. In the textural image of Fig. 9d, an SO type is shown. Here, quartz grains, probably with overgrowths, show sutured quartz grain limits in a three-dimensional structure in which new grains have formed. Unexpectedly, they are more numerous than we observed in thin section. Moreover, a few of the smaller grains are remnants of the original secondary grain framework. This structure, like the previous one, creates a stepped relief. Another sample of SO is shown in Fig. 9e and f. This variety is composed of bigger grains, which are extremely deformed. They generally present micro-stylolitic boundaries at which new grains have occasionally formed, creating a more compact material than other SO and especially the OO

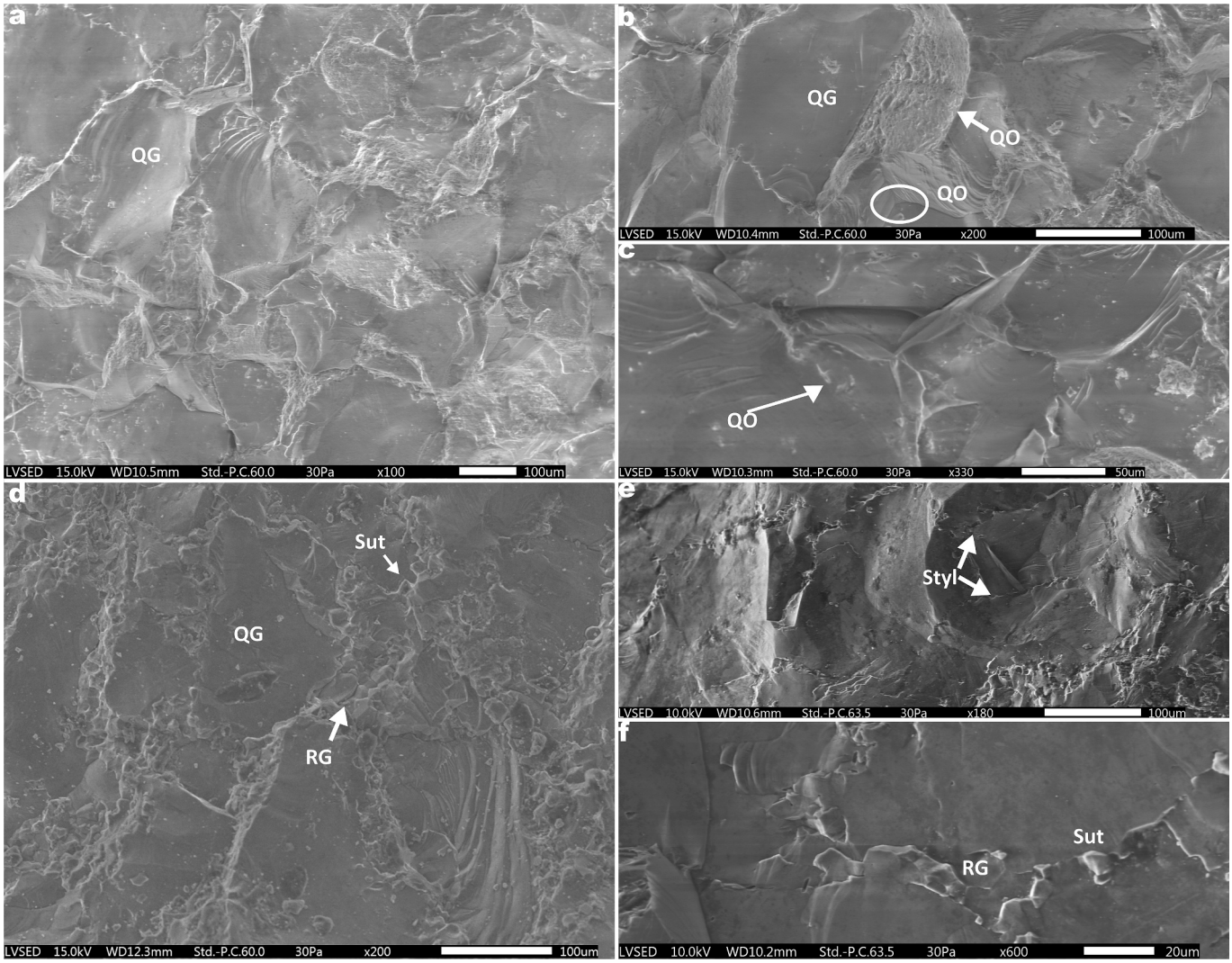

Fig. 9. Surfaces of OO and SO orthoquartzites observed with the SEM: a) Textural picture (100×) of DC-51-01, an OO type. Sample collected in a Carboniferous conglomerate in the Deva-Cares valley, Leon, Spain. b) Textural picture (200×) of DC51-01, an OO type showing concave-convex quartz grain limits and syntaxial overgrowths. c) Detailed picture (330×) of DC-51-01, an OO type, presenting quartz grain limit intersection and syntaxial overgrowths. d) Textural picture (200×) of DC-06-05, a fine-grained variety of SO type showing sutured quartz grain limits and a few recrystallised quartz grains. Sample taken in a Carboniferous conglomerate in the Deva-Cares valley, Cantabria, Spain. e) Textural picture (180×) of ATS-190, an SO type with bigger and more deformed crystals. Sample from the Mousterian level of El Arteu, Cantabria, Spain. f) Detailed picture (600×) of ATS-190 showing microstylolitic limits between quartz grains and the presence of a few recrystallised grains. QG: Quartz grain. QO: Quartz overgrowth. Sut: Suture. RG: Recrystallised grain. Styl: Microstylolitic grain limit.

types described previously.

Figs. 10 and 11 show the last three petrogenetic types –BQ, RQ, and MQ– observed with the SEM. All three samples present very gentle reliefs and relatively chaotic structures in which recrystallised grains play a prominent role. Fig. 10a and b present the textures of two different grain size varieties of the BQ type: coarse and fine, respectively. Both pictures show the sutured limits of old quartz grains and a high frequency of small recrystallised grains in which old grains float. The recrystallised quartz grains are very small and located at the limits of old grains (Fig. 10c). Fig. 10d and e correspond to an RQ type with a very gentle relief. Here, recrystallised quartz grains are situated not only at the limits of the original and extremely deformed quartz grains, but also in their inner parts. These newly formed grains are bigger than in the previous type, and they tend to accumulate in particular areas (Fig. 10f). Lastly, Fig. 11 presents three different samples of the MQ type in which a mosaic of quartz grains is displayed in an extremely smooth relief. The ease with which old and recrystallised quartz grains can be differentiated varies across the sample. Some quartz grain limits display sutures, whereas others show plain and concave-convex structures, which in some areas generate 120° triple points.

In sum, the imaging results demonstrate that the features that characterise each of the petrogenetic types are detectable with the SEM. This implies that the instrument is a powerful addition to the suite of non-destructive characterisation techniques. The SEM employed at the magnification range opted for here (mainly 100–700 ×) permits visualising features such as recrystallised grains, details of grain boundaries and of matrix and cement, and patterns of syntaxial overgrowth that are hard to detect reliably with optical microscopy and therefore usually analysed in thin section. In addition, in contrast with thin section petrography, it enables the evaluation of crack propagation with respect to structural features by providing a three-dimensional view of fracture surfaces.

5. Discussion: ongoing narrativesand future directions

The characterisation of quartzite artefacts using the aforementioned petrogenetic types constitutes a cornerstone to understand the management of the second most relevant lithic raw material in the

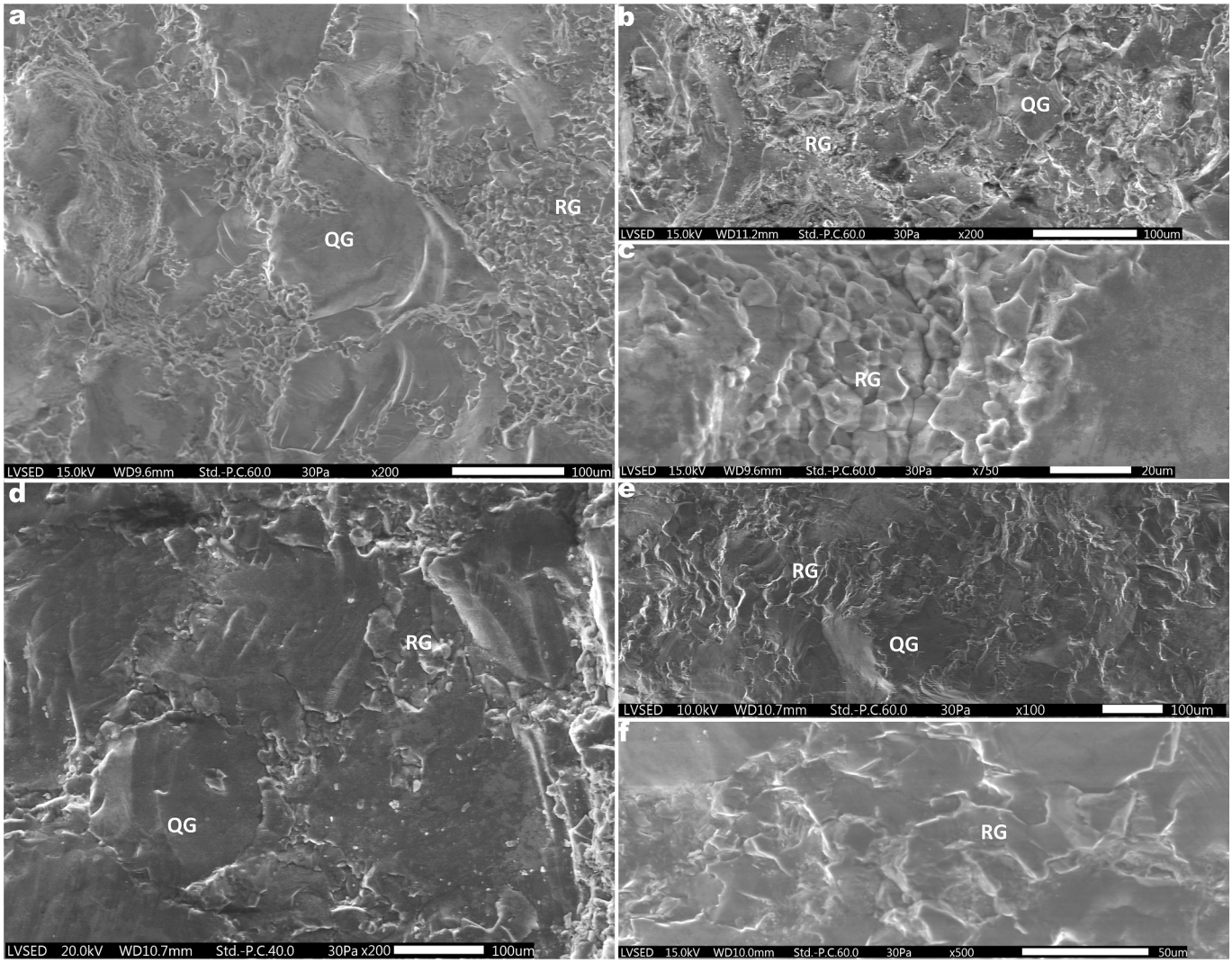

Fig. 10. Surfaces of BQ and RQ quartzites observed with the SEM: a) Textural picture (200×) of HA-5847, a BQ type with large and highly deformed quartz grains. Original large quartz grains co-occur with new small recrystallised quartz grains. Sample from the Mousterian level of El Habario, Spain. Middle Palaeolithic. b) Textural picture (200×) of DC-06-06, a BQ type with small quartz grains and limited presence of cement. Sutures are more obvious than in the previous sample. Sample taken in a Carboniferous conglomerate in the Deva-Cares valley, Cantabria, Spain. c) Detail (500×) of HA-5847 showing new recrystallised quartz grains at the limit between two original quartz grains. d) Textural picture (200×) of DC-75-02, an RQ type. Quartz grains are extremely deformed, broken and present sutured limits where new grains -bigger than in the previous samples- have formed. -Sample taken in a Carboniferous conglomerate in the Deva-Cares valley, Leon, Spain. e) Textural picture (100×) of banded Ci-55235 sample showing the RQ band. Sample from the Upper Solutrean level of El Cierro, Spain f) Detail (500×) of recrystallised quartz grains in sample ES-239, an RQ type from Level XIII of el Esquilleu, Cantabria, Spain. QG: Quartz grain. RG: Recrystallised grain.

Palaeolithic. In the last few years, our research team has shown how Neanderthals in Picos de Europa (Cantabrian Region, Iberia) managed petrogenetic types differently. The analysis of the Mousterian lithic artefacts from El Habario, El Arteu and El Esquilleu-XXII (Cantabria, Spain) unveiled different proportions of types at the three sites and when these assemblages were analysed technologically, metrically and typologically, we could infer common patterns such as 1) the more frequent exploitation of the more highly metamorphic types, associated with more complex management; 2) the use of (mobile) toolkits made from BQ, RQ and MQ types; and 3) the coexistence of complete and fragmentary operational sequences in different petrogenetic types. The latter differ at the three sites, according to the availability of petrogenetic types in the surroundings, the range of activities carried out at each site and, probably, the different knapping properties of each type (Prieto, 2018, 2022; Prieto et al., 2020).

Furthermore, we were able to geographically trace the origin of these quartzites thanks to the characterisation of quartzites deriving from potential procurement areas (massive outcrops, conglomerates and secondary deposits) and the analysis of cortical surfaces of the archaeological quartzite artefacts (Fernandes et al., 2007; Prieto et al., 2021c). In this case, the identification of the quartzite types was enhanced by the further classification of each type into varieties according to, for instance, quartz grain size and non-quartz mineral content. The mineralogical characterisation was strengthened with WD-XRF. At the aforementioned Middle Palaeolithic sites, quartzites were mainly collected locally, but some varieties were transported over distances exceeding 30 km across a rugged terrain that reflects the exploitation of low-altitude river banks and middle-altitude plateaus (Prieto et al., 2021c). For the Cantabrian Upper Palaeolithic, we also observed that quartzites were locally supplied, but longer mobility circuits (circa 50 km) were also detected, particularly at the so-called aggregation sites, such as the Asturian cave of Tito Bustillo (*Área de Estancia*) –Lower Magdalenian, *ca.* 18,000 cal BP-, where retouched tools were made from different types and varieties (Martín-Jarque et al., 2022).

The characterisation of strata with quartzites is also contributing to the understanding of the local and regional geology in the study regions.

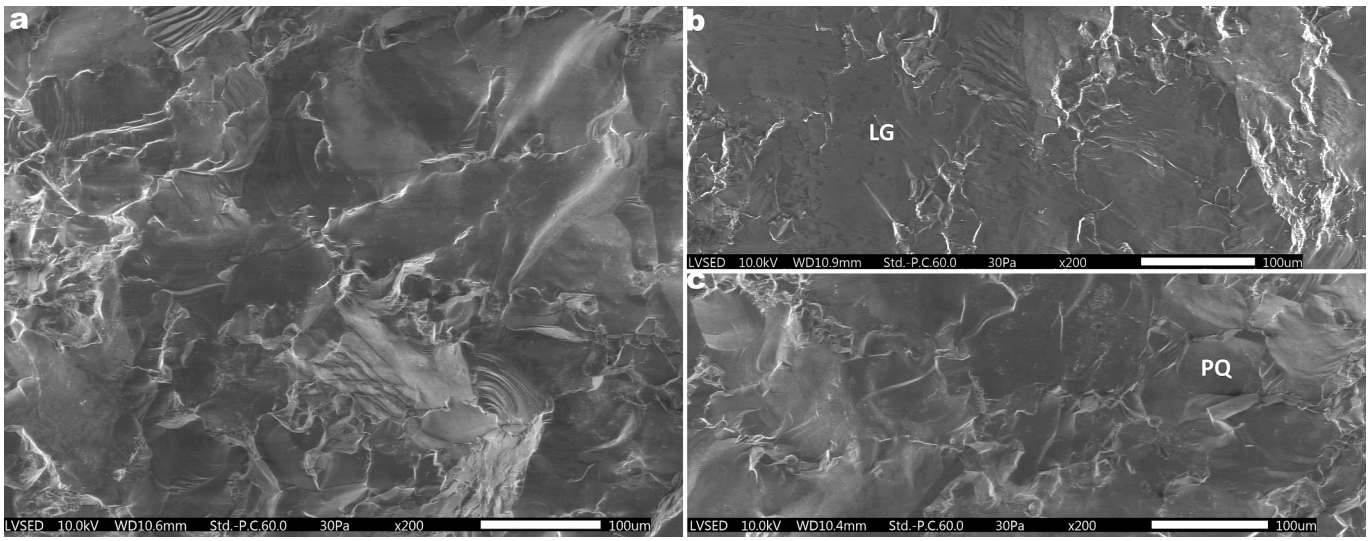

Fig. 11. Surfaces of MQ quartzites observed with the SEM: a) Textural picture (200×) of ES-411, an MQ type in which new recrystallised and old quartz grains cannot be distinguished. Sample from the Middle Palaeolithic Level XIII of el Esquilleu, Spain. b) Textural picture (100×) of CI-55325, showing the MQ band in the sample (compare Fig. 10e). Sample from the Solutrean level of El Cierro, Spain. c) Detail (200×) of ES-411. LG: Lobated quartz grain limit. PQ: Polygonised quartz grain.

This is the case for the Cantabrian Region, the Middle Rhine Valley, and, superficially, for the Arabian Peninsula and the Iberian Massif (Prieto, 2018; Prieto et al., 2024a, 2024b, 2021d). This, together with the description of quartzite facies in bedrock strata, the characterisation of cements in conglomerates, and the quantification of petrogenetic types of quartzites in consolidated and unconsolidated deposits, is shedding light on procurement and acquisition systems. Among others, we have been able to detect the quarrying of microcrystalline silica-cemented quartz-arenites (Pastoors et al., 2022) and different preferences in the selection of quartzites in river banks, especially when Cantabrian Middle Palaeolithic and Upper Palaeolithic levels are compared (Prieto, 2018; Prieto et al., 2022b, Prieto et al., in press).

Ongoing projects that are applying the petrogenesis of quartzite are geographically and chronologically widening our understanding of the procurement, transportation and management of quartzite throughout the Lower to the Upper Palaeolithic and from Central Europe to Southern Europe (Cristóbal et al., 2025; de Lombera-Hermida and Aldea-Moreira, 2023; Martín-Jarque et al., 2023; Prieto et al., 2024b), with further collaborative work in progress for Stone Age sites in southern Africa. Quartzite research in different parts of the world is also broadening our understanding of prehistoric resource management especially through the application of spectroscopic techniques, such as VNIR, LA-ICP-MS, and XRF (Favreau et al., 2021; Pitblado et al., 2012, Sherman III et al., 2024; Sjölander et al., 2024; Soto et al., 2020). This research has shown promising results in the East of Africa, the Scandinavian Peninsula and North America, but also underlined the high variability in rocks referred to as "quartzite" and the necessity of establishing coherent petrographic types to trace quartzite sources. This is particularly relevant for this rock and other silica-rich lithologies, whose composition is controlled by multiple factors, including petrogenetic processes.

The methodological potential in the application of petrogenesis and the different topics that can be addressed with it are wide and diverse. They include, among others, the knapping properties of different petrogenetic types and varieties, the visibility of technical stigmata on different quartzites, the application of transformative techniques to this raw material, and the variability in use-wear formation on different petrogenetic types (de la Peña et al., 2022; Eren et al., 2014; Pedergnana et al., 2017; Schmidt, 2021; Schmidt et al., 2024; Vaquero and Alonso-Fernández, 2020). We expect to address most of them in the following years thanks to the increased interest in this lithic resource, the maintenance and reinforcement of collaborations, and the application of new transdisciplinary approaches and methodologies.

Our exploratory SEM analysis of fracture surfaces of quartzite samples demonstrates that this technique allows obtaining a three-dimensional view of the diagnostic features of different quartzites previously observed in thin sections. It therefore represents a powerful complementary method for non-destructive characterisation of these rocks. Further work is required to understand how particular features such as syntaxial overgrowth of grains affect crack propagation and therefore the visual appearance of fracture surfaces, and how these features are best identified using scanning electron microscopy. Such investigations will also aid in linking relevant petrogenetic markers to the fracture mechanical properties of different quartzites for the benefit of lithic technological and functional analysis.

Finally, it is noteworthy that we limited the exploration here to magnifications below 1000×, focusing mostly on general textural features (magnifications 100–500×) to obtain comparisons with thin sections. The possibilities of the SEM in characterising e.g., matrix and cement in detail, or in detecting deformation or weathering features on constituent quartz grains, remain therefore underexplored.

6. Conclusions

A petrogenetic approach to archaeological quartzites presents a robust means to classify material and to understand the working properties of quartzites and their implications for prehistoric raw material economy. The methodological advances made in the recent years have expanded the scope of non-destructive characterisation of quartzites by revealing a systematic relationship between features observed in thin section and the properties of quartzite fracture surfaces, as observed under stereomicroscopes and digital microscopes. The exploratory scanning electron microscope study we presented here demonstrated that this instrument provides valuable additional data that allow detecting features usually only visible in thin section non-destructively and acquiring high-resolution topographic images that allow better understanding the links between the structural features and the fracture mechanical responses of different quartzites. This technique therefore holds significant future potential for the petrogenetic and archaeological analysis of quartzites as a part of a multi-scale and multi-instrument approach.

CRediT authorship contribution statement

Alejandro Prieto: Writing – review & editing, Writing – original draft, Methodology, Investigation, Formal analysis, Conceptualization. **Noora Taipale:** Writing – review & editing, Writing – original draft, Methodology, Investigation, Formal analysis, Conceptualization. **David Álvarez-Alonso:** Writing – review & editing, Validation, Data curation. **Esteban Álvarez-Fernández:** Writing – review & editing, Validation, Data curation. **Javier Baena-Preysler:** Writing – review & editing, Validation, Data curation. **Dries Cnuts:** Writing – review & editing, Methodology, Investigation, Formal analysis. **Ronè Oberholzer:** Writing – review & editing, Investigation, Formal analysis. **Andreas Pastoors:** Writing – review & editing, Validation, Data curation. **Veerle Rots:** Writing – review & editing, Supervision, Project administration, Methodology, Funding acquisition.

Acknowledgments

We offer our warm thanks to Lena Asryan for the organisation of the INSTONE workshop that paved the way for the collaborative exploratory study presented here. We are indebted to the Fund for Scientific Research (F.R.S.-FNRS), the University of Liège and the UR AAP for their financial support of this research. The authors thank MUPAC (Archaeological and Prehistorical Museum of Cantabria) and the CENIEH (Spanish National Centre for Human Evolution) for the permission to study the lithic archaeological material and the Department of Mineralogy and Petrology at the UPV/EHU for access to the laboratories and thin-section preparation. We also acknowledge the support given by Iñaki Yusta, from the aforementioned Department. Troisdorf project was funded by the Fritz Thyssen Foundation (20.15.0.021AA) and they gave support in obtained funds for thin petrographic analysis. Alejandro Prieto is researcher at the ERC-StG project SPEGEOCHERT funded by the European Union through the Horizon Europe program (ERC-2022-StG-101075451, SPEGEOCHERT). Views and opinions expressed are however those of the author(s) only and do not necessarily reflect those of the European Union or the European Research Council. Neither the European Union nor the granting authority can be held responsible for them. AP is part of the following Spanish Ministry of Science projects: Implementación de una infraestructura digital para litotecas arqueológicas en España- Digital Litho (RED2022-134387-T); Desafíos y oportunidades de investigación en los yacimientos arqueológicos pleistocenos de la cuenca de Guadix-Baza (Granada, España). Cuenca de Orce y Solana del Zamborino, ORCEpluSZ (PID2021-125098NB-100); Territorio y movilidad durante el Paleolítico superior en la encrucijada vasca, PALEOCROSS (PID2021-126937NB-100). In addition, he is a member of the Basque Research Group: Evolución humana, cambio climático y adaptación cultural en las sociedades preindustriales, GIZAPRE (IT-1435-22). We thank the two anonymous reviewers for their constructive comments and suggestions, which have helped improve the manuscript.

Data availability

Data will be made available on request.

References

Abrunhosa, A., Pereira, T., Márquez, B., Baquedano, E., Arsuaga, J.L., Pérez-González, A., 2019. Understanding Neanderthal technological adaptation at Navalmaíllo Rock Shelter (Spain) by measuring lithic raw materials performance variability. Archaeol. Anthropol. Sci. 11, 5949–5962. https://doi.org/10.1007/s12520-019-00826-3.

Adams, A.E., MacKenzie, W.S., Guilford, C., 1988. Atlas of sedimentary rocks under the microscope. ELBS, Essex.

Allaby, M., 2013. A Dictionary of Geology and Earth Sciences. Oxford University Press.

Arrizabalaga, A., Calvo, A., Elorrieta, I., Tapia, J., Tarriño, A., 2014. Where to and what for? Mobility patterns and the Management of Lithic Resources by Gravettian Hunter-Gatherers in the Western Pyrenees. J. Anthropol. Res. 70, 233–261. https://doi.org/10.3998/jar.0521004.0070.204.

Barkai, R., Gopher, A., 2009. Changing the face of the earth: human behaviour at Sede Ilan, an extensive lower-middle Paleolithic quarry site in Palestine. In: Adams, B., Blades, B. (Eds.), Lithic Materials and Palaeolithic Societies. Blackwell, Oxford, pp. 174–185.

Bastida, F., 1982. La esquistosidad primaria y las microestructuras de las cuarcitas en la zona Asturoccidental-leonesa. Trabajos De Geología 12, 159–185.

Belmiro, J., Terradas, X., Dominguez-Bella, S., Cascalheira, J., 2025. Within and beyond: Chert Procurement patterns during the Upper Palaeolithic in Southwesternmost Iberia. J. Paleolithic Archaeol. 8, 8. https://doi.org/10.1007/s41982-025-00209-2.

Blomme, A., Degryse, P., Van Peer, P., Elsen, J., 2012. The characterization of sedimentary quartzite artefacts from Mesolithic sites, Belgium. Geol. Belg. 15, 193–199.

Bucher, K., 2023. Introduction to metamorphic rocks, rock metamorphism, and metamorphic processes. In: Bucher, K. (Ed.), Petrogenesis of Metamorphic Rocks. Springer International Publishing, Cham, pp. 3–25, 10.1007/978-3-031-12595-9_1.

Calvo, A., Arrizabalaga, A., 2020. Piecing together a new mosaic: Gravettian lithic resources and economic territories in the Western Pyrenees. Archaeol. Anthropol. Sci. 12, 282–304. https://doi.org/10.1007/s12520-020-01231-x.

Cann, J.R., Renfrew, C., 1964. The characterization of obsidian and its application to the Mediterranean region. Proc. Prehistory Society 30, 111–133. https://doi.org/10.1017/S0079497X00015097.

Castro, A., 1989. Petrografía básica. Texturas, clasificación y nomenclatura de rocas. Paraningo, Madrid.

Cnudde, V., Dewanckele, J., De Kock, T., Boone, M., Baele, J.M., Crombé, P., Robinson, E., 2013. Preliminary structural and chemical study of two quartzite varieties from the same geological formation: a first step in the sourcing of quartzites utilized during the Mesolithic in northwest Europe. Geol. Belg. 16, 27–34.

Cristóbal, P., Navazo, M., Benito-Calvo, A., Alonso Alcalde, R., Prieto, A., 2025. Análisis y caracterización petrológica de las cuarcitas de la Cueva de Prado Vargas (Merindad de Sotoscueva, Burgos, España), in: Cortés-Sánchez, M., Simón-Vallejo, M., Pablos Fernández (Eds.), Neanderthals at the End of the World. New Perspectives for Iberia, SPAL Monografías Arqueológicas. Editorial Universidad de Sevilla, Sevilla, pp. 103–115.

Delvigne, V., Fernandes, P., Bindon, P., Bracco, J.P., Klaric, L., Lafarge, A., Langlais, M., Piboule, M., Raynal, J.P., 2019. Geo-resources and techno-cultural expressions in the south of the French Massif Central during the Upper Palaeolithic: determinism and choices. Antropol. Praehistorica 239, 39–55.

Doronicheva, E., Shackley, S., 2014. Obsidian exploitation strategies in the middle and upper paleolithic of the northern caucasus: new data from Mesmaiskaya Cave. PaleoAnthropol. 2014, 565–585.

Ebright, C., 1987. Quartzite petrography and its implications for Prehistoric use and archeological analysis. Archaeol. East. N. Am. 15, 29–45.

Eixea, A., Romagnoli, F., Bargalló, A., Gómez de Soler, B., Vaquero, M., Gema Chacón, M., 2020. Micro-lithic production at Abric Romaní levels L and Ob: Exploring economic and evolutionary implications for Neanderthal societies. J. Archaeol. Sci. Rep. 31, 102280. https://doi.org/10.1016/j.jasrep.2020.102280.

Eren, M.I., Roos, C.I., Story, B.A., von Cramon-Taubadel, N., Lycett, S.J., 2014. The role of raw material differences in stone tool shape variation: an experimental assessment. J. Archaeol. Sci. 49, 472–487. https://doi.org/10.1016/j.jas.2014.05.034.

Favreau, J., Carter, T., Soto, M., Bushozi, P.M., Magone, S., Durkin, P.R., Hubbard, S.M., Mercader, J., 2021. Early-Middle Pleistocene Raw Material Sourcing at Engaji Nanyori (Oldupai Gorge, Tanzania). In: Gómez de Soler, B., Soto, M., Chacón, M.G., Soares Remiseiro, M. (Eds.), Presented at the Rock and Roll: 13th International Symposium on Knappable Materials, Adhoc Cultura, Tarragona, Spain, pp. 68–69.

Favreau, J., Soto, M., Nair, R., Bushozi, P.M., Clarke, S., DeBuhr, C.L., Durkin, P.R., Hubbard, S.M., Inwood, J., Itambu, M., Larter, F., Lee, P., Marr, R.A., Mwambwiga, A., Patalano, R., Tucker, L., Mercader, J., 2020. Petrographic Characterization of Raw Material sources at Oldupai Gorge, Tanzania. Front. Earth Sci 8. https://doi.org/10.3389/feart.2020.00158.

Fernandes, P., Le Bourdonnec, F.-X., Raynal, J.-P., Poupeau, G., Piboule, M., Moncel, M.-H., 2007. Origins of prehistoric flints: the neocortex memory revealed by scanning electron microscopy. C.R. Palevol 6, 557–568. https://doi.org/10.1016/j.crpv.2007.09.015.

Fernandes, P., Raynal, J.-P., Moncel, M.-H., 2008. Middle Palaeolithic raw material gathering territories and human mobility in the southern Massif Central, France: first results from a petro-archaeological study on flint. J. Archaeol. Sci. 35, 2357–2370. https://doi.org/10.1016/j.jas.2008.02.012.

Floss, H., 1994. Rohmaterialversorgung im Paläolithikum des Mittelrheingebietes. Dissertation Universität zu Köln, Verlag des Römisch-Germanischen Zentralmuseums. Monographien des Römisch-Germanischen Zentralmuseums. Habelt, Mainz.

Folk, R., 1974. Petrology of Sedimentary Rocks. Hemphill Publishing Company, Austin, Texas.

Gómez de Soler, B., Soto, M., Vallverdú, J., Vaquero, M., Bargalló, A., Chacón, M.G., Romagnoli, F., Carbonell, E., 2020. Neanderthal lithic procurement and mobility patterns through a multi-level study in the Abric Romaní site (Capellades, Spain). Quat. Sci. Rev. 237, 106315. https://doi.org/10.1016/j.quascirev.2020.106315.

Hirth, G., Teyssier, C., Dunlap, J., 2001. An evaluation of quartzite flow laws based on comparisons between experimentally and naturally deformed rocks. Int. J. Earth Sci. 90, 77–87. https://doi.org/10.1007/s005310000152.

Hirth, G., Tullis, J., 1992. Dislocation creep regimes in quartz aggregates. J. Struct. Geol. 14, 145–159.

Howard, J.L., 2005. The quartzite problem revisited. J. Geol. 113, 707–713. https://doi.org/10.1086/449328.

Knutsson, H., Knutsson, K., Molin, F., Zetterlund, P., 2016. From flint to quartz: Organization of lithic technology in relation to raw material availability during the

pioneer process of Scandinavia. Quat. Int. 424, 32–57. https://doi.org/10.1016/j.quaint.2015.10.062.
Krynine, P.D., 1948. The megascopic study and field classification of sedimentary rocks. J. Geol. 56, 130–165.
Legg, R., Neilson, J., Demel, S., 2020. Novel use of cathodoluminescence to identify differences in source rocks for Late Paleoindian quartzite tools 62, 875–887. 10.1111/arcm.12568.
de Lombera-Hermida, A., Aldea-Moreira, X., 2023. Nuevas aportaciones al estudio de las materias primas en el Noroeste peninsular. La gestión de las materias primas en los yacimientos de Valverde (Monforte de Lemos, Lugo) y Cova Eirós (Triacastela, Lugo), in: Las Materias Primas Líticas En La Prehistoria Del Pirineo y La Región Cantábrica, Veleia: Series Minor. Servicio Editorial de la Universidad del País Vasco, Vitoria-Gasteiz, pp. 17–48.
de Lombera-Hermida, A., Rodríguez-Rellán, C., 2016. Quartzes matter. Understanding the technological and behavioural complexity in quartz lithic assemblages. Quat. Int. 424, 2–11. https://doi.org/10.1016/j.quaint.2016.11.039.
Maier, A., Sauer, F., Bergsvik, K.A., 2022. Transport patterns as heuristic testing variables for the social coherence of taxonomic units at different spatial scales. J. Paleolithic Archaeol. 5, 8. https://doi.org/10.1007/s41982-022-00120-0.
Martín-Jarque, S., Herrero-Alonso, D., Tarriño, A., López-Tascón, C., Prieto, A., Bécares, J., Álvarez-Fernández, E., 2022. Determination of lithic raw materials in Cantabrian Spain during Greenland Stadial 2: the Magdalenian of Tito Bustillo Cave (Ribadesella, Asturias). J. Archaeol. Sci. Rep. 103678. https://doi.org/10.1016/j.jasrep.2022.103678.
Martín-Jarque, S., Tarriño, A., Delclòs, X., García-Alonso, B., Peñalver, E., Prieto, A., Álvarez-Fernández, E., 2023. Les silex et autres matières premières comme preuves de contacts entre les groupes de chasseurs-cueilleurs pendant le Paléolithique supérieur de la région cantabrique (nord de l'Espagne) : synthèse de l'information disponibl. L'anthropologie 127, 103092. https://doi.org/10.1016/j.anthro.2022.103092.
Mayor, A., Sossa-Ríos, S., Molina, F.J., Pérez, L., Galván, B., Mallol, C., Hernández, C.M., 2022. An instance of Neanderthal mobility dynamics: a lithological approach to the flint assemblage from stratigraphic unit viii of El Salt rockshelter (Alcoi, eastern Iberia). J. Archaeol. Sci. Rep. 44, 103544. https://doi.org/10.1016/j.jasrep.2022.103544.
McHenry, L.J., de la Torre, I., 2018. Hominin raw material procurement in the Oldowan-Acheulean transition at Olduvai Gorge. J. Hum. Evol. 120, 378–401. https://doi.org/10.1016/j.jhevol.2017.11.010.
Nash, D.J., Ciborowski, T.J.R., Coulson, S.D., Staurset, S., Burrough, S.L., Mothulatshipi, S., Thomas, D.S.G., 2022. Mapping Middle Stone Age human mobility in the Makgadikgadi Pans (Botswana) through multi-site geochemical provenancing of silcrete artefacts. Quat. Sci. Rev. 297, 107811. https://doi.org/10.1016/j.quascirev.2022.107811.
Orange, M., Le Bourdonnec, F.-X., Berthon, R., Mouralis, D., Gratuze, B., Thomalsky, J., Abedi, A., Marro, C., 2021. Extending the scale of obsidian studies: Towards a high-resolution investigation of obsidian prehistoric circulation patterns in the southern Caucasus and north-western Iran. Archaeometry 63, 923–940. https://doi.org/10.1111/arcm.12660.
Ortiz, I., Baena, J., 2016. Did Stones Speak About People? Flint catchment and Neanderthal behavior from Area 3 (Cañaveral, Madrid-Spain). Quaternary International, 10.1016/j.quaint.2016.01.019.
Passchier, C.W., Trouw, R.A.J., 2005. Microtectonics, 2nd ed. Springer-Verlag, Berlin/Heidelberg. 10.1007/3-540-29359-0.
Pastoors, A., Kehl, M., Prieto, A., Henselowski, F., King, G., Peresani, M., Vaquero, M., Claßen, E., 2022. New light on the Middle Palaeolithic quartzite extraction site Troisdorf-Ravensberg (North Rhine-Westphalia, Germany). Bonner Jahrbücher 221, 3–64.
Pedergnana, A., García-Antón, M.D., Ollé, A., 2017. Structural study of two quartzite varieties from the Utrillas facies formation (Olmos de Atapuerca, Burgos, Spain): from a petrographic characterisation to a functional analysis design. Quat. Int. 433, 163–178. https://doi.org/10.1016/j.quaint.2015.06.031.
Pedergnana, A., Ollé, A., Borel, A., Moncel, M.-H., 2018. Microwear study of quartzite artefacts: preliminary results from the Middle Pleistocene site of Payre (South-eastern France). Archaeol. Anthropol. Sci. 10, 369–388. https://doi.org/10.1007/s12520-016-0368-2.
de la Peña, P., Thomas, M., Molefyane, T.R., 2022. Particle size distribution: an experimental study using southern african reduction methods and raw materials. PLoS One 17, e0278867. https://doi.org/10.1371/journal.pone.0278867.
Pettijohn, F.J., 1954. Classification of sandstones. J. Geol. 62, 360–365. https://doi.org/10.2307/30065017.
Pitblado, B., Cannon, M., Neff, H., Dehler, C., Nelson, S., 2012. LA-ICP-MS Analysis of Quartzite from the Upper Gunnison Basin, Colorado. J. Archaeol. Sci. 40, 2196–2216.
Prieto, A., 2018. Procurement and management of quartzite in the Cantabrian Region: the Middle and Upper Palaeolithic in the Deva. Departamento de Geografía, Prehistoria y Arqueología. Universidad del País Vasco, Cares and Güeña Valleys (PhD).
Prieto, A., 2022. La cuarcita en el Cantábrico central: aplicación de una metodología transdisciplinar y multifocal a la otra materia prima lítica. Arkeogazte Revista 12, 99–128.
Prieto, A., Aldea-Moreira, X., Arzarello, M., Berruti, G.L.F., Caracausi, S., Daffara, S., De la Peña, P., Favreau, J., García-Rojas, M., Huysecom, E., Janardhana, B., Kumar Jha, D., Lahari, L., Molefyane, T.R., Pruvost, C., Rodríguez-Álvarez, X.P., Thomas, M., Vaishnav, H.K., Villeneuve, Q., de Lombera-Hermida, A., 2022a. How to deal with an elephant in the room? Understanding "non-flint" raw materials: characterisation and technological organisation. Revista ArkeoGazte 12, 73–98.
Prieto, A., Arrizabalaga, A., Yusta, I., 2021. Lithic Raw Material in the Cantabrian Region: Dialectical relationship between flint and quartzite in the Palaeolithic record. J. Lithic Studies 8, 31. https://doi.org/10.2218/jls.4334.
Prieto, A., Cristóbal, P., Hilbert, Y., Crassard, R., Schiettecatte, J., 2024a. Petrographic characterisation of Arabian Quartz-Arenites: Unveiling petrogenesis and weathering processes of abiotic prehistoric resources. 10.5281/zenodo.14179003.
Prieto, A., Cristóbal, P., Llamazares González, J., Cuartero, F., 2024b. The quartzite and quartz reference collection from the CENIEH (Spanish National Research Centre on Human Evolution), Spain: an Online Database for Characterising a Wide Diversity of Lithic Raw Materials. J. Open Archaeol. Data 12, 10. https://doi.org/10.5334/joad.128.
Prieto, A., García-Rojas, M., Sánchez, A., Calvo, A., Domínguez-Ballesteros, E., Ordoño, J., García Collado, M.I., 2016. Stones in Motion: cost units to understand flint procurement strategies during the Upper Palaeolithic in the south-western Pyrenees using GIS. J. Lithic Studies 3, 133–160. https://doi.org/10.2218/jls.v3i1.1310.
Prieto, A., Sánchez, A., de Lombera Hermida, A., Calvo, A., 2023. Construyendo la sección de cuarcitas en la Litoteka de la UPV/EHU: desde la prospección hasta su archivo. In: Prieto, A., de Lombera-Hermida, A., Calvo, A., Domínguez-Ballesteros, E., Arrizabalaga, A. (Eds.), Las Materias Primas Líticas En La Prehistoria Del Pirineo y La Región Cantábrica, Veleia: Series Minor. Servicio Editorial de la Universidad del País Vasco, Vitoria-Gasteiz, pp. 303–332.
Prieto, A., Álvarez-Alonso, D., Arrizabalaga, A., Calvo, A., Yravedra Sainz de los Terreros, J., Yusta, I., in press. The role of quartzite in a Gravettian short-term camp: Procurement and management strategies at Level 6, Coímbre Cave (Cantabrian Region, Iberian Peninsula). J. Archaeol. Sci.: Rep.
Prieto, A., Yusta, I., Arrizabalaga, A., 2020. From petrographic analysis to stereomicroscopic characterisation: a geoarchaeological approach to identify quartzite artefacts in the Cantabrian Region. Archaeol. Anthropol. Sci. 12, 32. https://doi.org/10.1007/s12520-019-00981-7.
Prieto, A., Yusta, I., Arrizabalaga, A., 2019. Defining and Characterizing Archaeological Quartzite: Sedimentary and Metamorphic Processes in the Lithic Assemblages of El Habario and El Arteu (Cantabrian Mountains, Northern Spain). Archaeometry 61, 14–30. https://doi.org/10.1111/arcm.12397.
Prieto, A., Yusta, I., García-Rojas, M., Arrizabalaga, A., Baena Preysler, J., 2022b. Quartzite procurement, not only in fluvial deposits: raw material characterisation of the lithic assemblage from Level XXII-R at El Esquilleu, Cantabrian Region. Spain. Journal of Lithic Studies 8, 34. https://doi.org/10.2218/jls.4492.
Prieto, A., Yusta, I., García-Rojas, M., Arrizabalaga, A., Baena Preysler, J., 2021c. Quartzite procurement in conglomerates and deposits: Geoarchaeological characterization of potential catchment areas in the central part of the Cantabrian Region, Spain. Geoarchaeology 36, 490–510. https://doi.org/10.1002/gea.21838.
Prieto, A., Yusta, I., Pastoors, A., Claßen, E., 2021d. Petrological characterisation of the "Tertiary quartzites" from the site of Troisdorf-Ravensberg (North Rhine-Westphalia, Germany): first insights in Middle Palaeolithic outcrop exploitation. Quartär 66, 33–50. https://doi.org/10.7485/QU66_2.
Rios-Garaizar, J., 2020. Microlithic lithic technology of Neandertal shellfishers from El Cuco rockshelter (Cantabrian Region, northern Spain). J. Archaeol. Sci. Rep. 30, 102201. https://doi.org/10.1016/j.jasrep.2020.102201.
Roy, M., Mora, R., Plasencia, F.J., Martínez-Moreno, J., Benito-Calvo, A., 2017. Quartzite selection in fluvial deposits: the N12 level of Roca dels Bous (Middle Palaeolithic, southeastern Pyrenees). Quat. Int. 435, 49–60. https://doi.org/10.1016/j.quaint.2015.09.010.
Sánchez de la Torre, M., Le Bourdonnec, F.-X., Gratuze, B., 2017. Reconsidering prehistoric chert catchment sources: new data from the Central Pyrenees (Western Europe). Archaeol. Anthropol. Sci. https://doi.org/10.1007/s12520-017-0581-7.
Sánchez de la Torre, M., Utrilla, P., Montes, L., Domigo, R., Le Bourdonnec, F.X., Gratuze, B., 2020. Characterizing the lithic raw materials from Fuente del Trucho (Asque-Colungo, Huesca): New data about Palaeolithic human mobility in north-east Iberia. Archaeometry 247–265. https://doi.org/10.1111/arcm.12612.
Schmidt, P., 2021. Steak tournedos or beef Wellington: an attempt to understand the meaning of Stone Age transformative techniques. Human. Soc. Sci. Commun. 8, 280. https://doi.org/10.1057/s41599-021-00971-y.
Schmidt, P., Pappas, I., Porraz, G., Berthold, C., Nickel, K.G., 2024. The driving force behind tool-stone selection in the African Middle Stone Age. Proc. Natl. Acad. Sci. 121, e2318560121. https://doi.org/10.1073/pnas.2318560121.
Sherman, S.P., Parish, R.M., Kwon, Y., Meredith, S., Johnson, D., 2024. Non-destructively characterizing sandstones, orthoquartzites, agates, and petrified wood for provenance research: Perspectives from the Southeastern Coastal Plain, United States. Geoarchaeology 39, 628–644. https://doi.org/10.1002/gea.22018.
Sjölander, M., Linderholm, J., Geladi, P., Buckland, P.I., 2024. Quartzite complexities: Non-destructive analysis of bifacial points from Västerbotten, Sweden. J. Archaeol. Sci.: Reports 53, 104381. https://doi.org/10.1016/j.jasrep.2024.104381.
Skolnick, H., 1965. The quarzite problem. J. Sediment. Petrol. 35, 12–21.
Soto, M., Favreau, J., Campeau, K., Carter, T., Abtosway, M., Bushozi, P.M., Clarke, S., Durkin, P.R., Hubbard, S.M., Inwood, J., Itambu, M., Koromo, S., Larter, F., Lee, P., Mwambwiga, A., Nair, R., Olesilau, L., Patalano, R., Tucker, L., Mercader, J., 2020. Fingerprinting of quartzitic outcrops at Oldupai Gorge, Tanzania. J. Archaeol. Scie.: Reports 29, 102010. https://doi.org/10.1016/j.jasrep.2019.102010.
Sternke, F., 2007. The German quartzite palaeolithic: an exploration of late middle pleistocene hominid behaviour in relation to the utilization of non-flint raw material. Lithic Technol. 32, 115–130. https://doi.org/10.1080/01977261.2007.11721047.
Stipp, M., Stünitz, H., Heilbronner, R., Schmid, S.M., 2002a. Dynamic recrystallization of quartz: Correlation between natural and experimental conditions. Geol. Soc. Lond. Spec. Publ. 200, 171–190.

Stipp, M., Stünitz, H., Heilbronner, R., Schmid, S.M., 2002b. The eastern Tonale fault zone: a "natural laboratory" for crystal plastic deformation of quartz over a temperature range from 250 to 700 °C. J. Struct. Geol. 24, 1861–1884. https://doi.org/10.1016/S0191-8141(02)00035-4.

Stipp, M., Tullis, J., 2003. The recrystallized grain size piezometer for quartz. Geophys. Res. Lett. 30, n/a-n/a. https://doi.org/10.1029/2003GL018444.

Stipp, M., Tullis, J., Scherwath, M., Behrmann, J.H., 2010. A new perspective on paleopiezometry: Dynamically recrystallized grain size distributions indicate mechanism changes. Geology 38, 759–762. https://doi.org/10.1130/G31162.1.

Tarbuck, E.J., Lutgens, F.K., Tasa, D., 2005. Ciencias de la Tierra. Pearson Educación, Madrid.

Tarriño, A., Ábalos, B., Puelles, P., Eguiluz, L., Díez-Martín, F., 2023. The crystalline quartz-rich raw material from Olduvai Gorge (Tanzania): why is it called quartzite when it should be called quartz? Archaeol. Anthropol. Sci. 15, 78. https://doi.org/10.1007/s12520-023-01774-9.

Tarriño, A., Elorrieta, I., García-Rojas, M., 2016. Flint as raw material in prehistoric times: Cantabrian Mountain and Western Pyrenees data. Quat. Int. 364, 94–108. https://doi.org/10.1016/j.quaint.2014.10.061.

Vaquero, M., Alonso-Fernández, E.S., 2020. Technological changes and chrono-cultural boundaries: the role of expedient technologies in the upper paleolithic. J. Archaeol. Sci. Rep. 31, 102346. https://doi.org/10.1016/j.jasrep.2020.102346.

Vaquero, M., Romagnoli, F., Bargalló, A., Chacón, M.G., Gómez de Soler, B., Picin, A., Carbonell, E., 2019. Lithic refitting and intrasite artifact transport: a view from the Middle Paleolithic. Archaeol. Anthropol. Sci. 11, 4491–4513. https://doi.org/10.1007/s12520-019-00832-5.

Veldeman, I., Baele, J.M., Goemaere, E., Deceukelaire, M., Dusar, M., De Doncker, H., 2012. Characterizing the hypersiliceous rocks of Belgium used in (pre-)history: a case study on sourcing sedimentary quartzites. J. Geophys. Eng. 9, 118–128. https://doi.org/10.1088/1742-2132/9/4/S118.

Viallet, C., Fernandes, P., Lahaye, C., Lebrun, B., Rué, M., Tallet, P., 2024. Une nouvelle occurrence de l'Acheuléen pyrénéo-garonnais et la question de la régionalisation des productions lithiques à la fin du Pléistocène moyen : le site du Cassé à Cornebarrieu (Haute-Garonne). L'anthropologie 128, 103236. https://doi.org/10.1016/j.anthro.2024.103236.

Villeneuve, Q., Faivre, J.-P., Turq, A., Guadelli, J.-L., 2019. Étude techno-économique du Moustérien de Pradayrol (Caniac-du-Causse, lot) : entre mobilité des ressources lithiques et adaptation aux matériaux locaux, un exemple de gestion complémentaire des quartz et silex au Paléolithique moyen récent en Querc. C.R. Palevol 18, 251–267. https://doi.org/10.1016/j.crpv.2018.10.002.

Wentworth, C.K., 1922. A scale of grade and class terms for clastic sediments. J. Geol. 30, 377–392.

Wilson, C.J.L., 1973. The prograde microfabric in a deformed quartzite sequence, Mount Isa, Australia. Tectonophysics 19, 39–81. https://doi.org/10.1016/0040-1951(73)90142-X.

Yardley, B.W.D., Mackenzie, W.S., Guilford, C., 1990. Atlas of metamorphic rocks and their textures. Longman Scientific & Technical, Essex. https://doi.org/10.1111/j.1365-3121.1991.tb00877.x.

Yezad, P., 2023. Scratching the surface(s): examining the complexity of geological contexts for the Palaeolithic of the Sonar Basin, Madhya Pradesh. Geol. Soc. Lond. Spec. Publ. 515, 279–301. https://doi.org/10.1144/SP515-2020-234.

Zilhão, J., Angelucci, D.E., Le Bourdonnec, F.-X., Lucena, A., Martín-Lerma, I., Martínez, S., Matias, H., Villaverde, V., Zapata, J., 2021. Obsidian in the Upper Palaeolithic of Iberia. Antiquity 95, 865–884. 10.15184/aqy.2021.85.